

**SYNTHESIS AND CHARACTERIZATION
OF SILICIOUS GEOTHERMAL SCALES AND
INHIBITION OF THEIR FORMATION BY
ORGANIC COMPOUNDS**

**A Thesis Submitted to the Graduate School of Engineering and
Science of İzmir Institute of Technology in Partial Fulfillment of the
Requirement for the Degree of Master of Science**

MASTER OF SCIENCE

In Chemistry

**by
Irmak TUNÇ**

**July 2014
İZMİR**

We approve the thesis of **Irmak TUNÇ**

Examining Committee Members:

Prof. Dr. Mehtap EMİRDAĞ EANES

Department of Chemistry, İzmir Institute of Technology

Prof. Dr. Alper BABA

Department of Civil Engineering, İzmir Institute of Technology

Prof. Dr. Mustafa M. DEMİR

Department of Material Science and Engineering, İzmir Institute of Technology

07 July 2014

Prof. Dr. Mustafa M. DEMİR

Supervisor, Department of Material Science and Engineering, İzmir Institute of Technology

Prof. Dr. Ahmet E. EROĞLU

Head of the Department of Chemistry

Prof. Dr. R. Tuğrul SENGER

Dean of the Graduate School of Engineering and Sciences

ACKNOWLEDGEMENTS

Firstly, I would like to express my appreciation to my supervisor Prof. Dr. Mustafa M. DEMİR for giving me the opportunity to carry out my graduate study.

I would like to express my appreciations to Center For Materials Research and Environmental Development Application and Research Center specialists, especially Sanem Ezgi KINAL.

I would like to thank to Prof. Dr. Alper BABA for helping me at writing my thesis.

As well as, I would like to thank all of my friends in IYTE.

Finally, I would like to thank my parents for their support. I dedicate my thesis to my family.

ABSTRACT

SYNTHESIS AND CHARACTERIZATION OF SILICIOUS GEOHERMAL SCALES AND INHIBITION OF THEIR FORMATION BY ORGANIC COMPOUNDS

Geothermal energy is the thermal energy generated and stored in the earth and geothermal source, provides most reliable, sustainable, cost effective and environmentally friendly method among other energy sources. However, silicate scale deposits such as metal-silicate compounds present important challenges for geothermal energy fields. While the mineral-rich ground water comes to surface, due to the decrease in pressure, acidity and temperature the solubility of silicon and minerals in water decrease and precipitation occurs. In geothermal systems, a layer forms because of the precipitation at the inner surface of pipes. This layer is called scale or deposit. Eventually, the diameter of the pipe decreases upon the occupation of scales in the pipe, therefore the efficiency of electricity production reduces.

In this study, artificial scale was created to test inhibitors in the laboratory. For this, the structure of the scale formed in the geothermal fields was analyzed and it was synthesized in laboratory. Then, method was optimized to determine the substances which can act as inhibitor. Later, the effectiveness of the substances which may act on the metal-silicate formation was tested. Polyacrylamide, Poly(acrylamide-co-diallyl dimethyl ammonium chloride), Polyvinylpyrrolidone, Polyacrylicacid was tried at different dosage and for different reaction time. Polyacrylicacid provides remarkable inhibition efficiency at low dosage. At 60 ppm dosage level, ~180 ppm increase is seen at soluble silica level. As a result of these tests, a new inhibitor or dispersant can be developed based on the molecular structure of effective inhibitors.

ÖZET

SİLİSYUM ZENGİN JEOTERMAL KABUĞUN SENTEZİ, KARAKTERİZASYONU VE OLUŞUMUNUN ORGANİK BİLEŞİKLERLE ENGELLENMESİ

Hem ekonomik hem de çevreye zararı çok az olan sürdürülebilir enerji kaynaklarının en etkin olanlarından bir tanesi jeotermal enerjidir. Jeotermal enerji üretim tesislerinin en önemli işletimsel problemi kabuklaşmadır. Mineralce zengin olan yeraltı suları, yeryüzüne çıkarken basıncın asitliğin ve sıcaklığın düşmesi ile sudaki silisyum ve minerallerin çözünürlüğü düşmekte ve çökeltme meydana gelmektedir. Jeotermal sistemlerde boru içerisinde, çökeltmeden dolayı bir tabaka meydana gelir. Bu tabakaya kabuk (scale) ya da depozit denilmektedir. Bu kabuk tesisin boru sistemlerinin iç çapını küçülttüğü için elektrik üretim verimliliğini azaltmaktadır.

Bu projede, laboratuvar koşullarında inhibitör maddelerin test edilmesi için yapay silikat sentezi yapılmıştır. Bunun için öncelikle jeotermal enerji üretim tesisinden alınan örnekler detaylı olarak incelenmiştir. Ve bu yapının benzeri laboratuvar da geri soğutma düzeneğinde sentezlenmiştir. Sentezlenen bu yapının inhibitör testlerinde kullanılabilmesi için metot optimizasyonu yapılmıştır. Daha sonra farklı polimer maddelerin metal-silikat oluşumu üzerinde inhibitör etkileri test edilmiştir. Poliakrilamid, Poli(akrilamid-co-diiallil dimetil amonyum klorit), Polivinilpirrolidon, Poliakrilik asit'in farklı konsantrasyonları ve farklı reaksiyon süreleri test edilmiştir. Bu polimerler arasından Poliakrilikasit düşük konsantrasyonda katım ile kayda değer etkinlik göstermiştir. 60 ppm Poliakrilikasit katımı ile çözünmüş silika konsantrasyonunda ~180 ppm artış görülmüştür. Bu çalışmaların sonucunda inhibitör ya da dispersant etkisi gösterebilecek yeni bir yapının sentezine ışık tutabilecek bilgiler elde edilmiştir.

To my family...

TABLE OF CONTENTS

LIST OF FIGURES	ix
LIST OF TABLES	xi
CHAPTER 1. INTRODUCTION	1
1.1. Geothermal Energy and Scaling Problem	1
1.2. Types of Scaling	2
1.3. Literature Review	2
1.3.1. Mechanism of Scaling	2
1.3.2. Inhibitor Chemistry	7
1.4. Aim of the Study.....	17
CHAPTER 2. EXPERIMENTAL SECTION.....	19
2.1. Chemicals and Reagents	19
2.2. Sampling and Characterization of Natural Silicate	19
2.3. Synthesis of Artificial Silicate	20
2.4. Inhibitor Tests	22
2.5. Characterization Tools and Applied Methods	22
2.5.1. Scanning Electron Microscopy (SEM)	22
2.5.2. X-ray Diffractometry (XRD).....	23
2.5.3. X-ray Fluorescence (XRF)	23
2.5.4. Inductively Coupled Plasma Mass Spectrometry.....	23
2.5.5. Zeta Sizer	24
2.5.6. Visible and Ultraviolet Spectroscopy.....	24
2.5.7. Silicomolibdate Spectrophotometric Method	24
CHAPTER 3. RESULTS AND DISCUSSIONS.	24
3.1. Identification of Natural Scale.....	26
3.2. Fabrication of Synthetic Scale	26
3.3. Inhibition of Scale by Polymeric Compounds.....	31
3.3.1. Polyacrylamide.....	33

3.3.2. Poly(acrylamide-co-diallyl dimethyl amonium chloride).....	36
3.3.3. Polyvinylpirrolidone	38
3.3.4. Polyacrylicacid	40
3.3.5. Molecular Weight on Parameter	42
CHAPTER 4. CONCLUSION	46
REFERENCES	48

LIST OF FIGURES

<u>Figure</u>	<u>Page</u>
Figure 1.1. Scaling problem in some geothermal fields	1
Figure 1.2. Polymerization reaction of ortho silicic acid.....	3
Figure 1.3. Schematic view of well.	3
Figure 1.4. Schematic presentation of formation of metal-silicate particle.....	4
Figure 1.5. Tentative explanation for the formation of bulk scale	6
Figure 1.6. Molecular structure of (a) PAMAM (Generation-1) and (b) PAMAM (Generation-2).....	7
Figure 1.7. Solubility dependence of SiO ₂ on PAMAM-1.0 dendrimer dosage	9
Figure 1.8. Solubility dependence of SiO ₂ on PAMAM-2.0 dendrimer dosage	9
Figure 1.9. (a) Ethylene diamine tetra(methylenephosphonic acid), (b) 1-Hydroxy ethyl diene-1,1-diphosphonic acid, (c) Hydroxy ethylene phosphono acetic acid, (d) Hidroxy ethylene amine phosphonic acid, (e) Hexamethylene-N,N',N',N'-diamine tetramethylenephosphonic acid, (f) Amino trimethylene phosphonic acid, (g) Amino-tris (methylenephosphonate).	10
Figure 1.10. (a) Polyacrylic acid, (b) Polymethacrylic acid, (c) Acrylic acid/ methacrylic acid copolymer, (d) 2-phosphonobutane-1,2,4-tricarboxylic acid, (e) Carboxymethylinulin, (f) Polyethyloxazolin (AQUAZOL)	11
Figure 1.11. Effectiveness test of polyacrilate.....	13
Figure 1.12. Effectiveness test of 2-phosphonobutane-1,2,4- tricarboxylic acid	13
Figure 1.13. (a) PALAM, (b) PAMALAM, (c) Polyethyleneimin, (d) CATIN	14
Figure 1.14. Solubility test of silicate in presence of 20 ppm PALAM	15
Figure 1.15. Solubility test of silicate in the presence of PALAM and CATIN.....	15
Figure 1.16. Effectiveness test of polyethyleneimine.....	16
Figure 1.17. Location of Tuzle GEP Co.	18
Figure 2.1. Schematic illustration of reflux	20
Figure 2.2. Schematic view of procedure for the formation of synthetic scale	21
Figure 3.1. Morphological features of (a) natural scale and (b) artificial scale.....	27
Figure 3.2. XRD patterns of natural scale and artificial scale	27

Figure 3.3. UV results of change that observe during preparation sample while Fe-Mg-Ca Silicate synthesis. (A) Just salt solution, (B) salt+ Na-Silicate solution before reaction, (C) decantate after reaction	29
Figure 3.4. (A) Before centrifuge and (B) after centrifuge.....	30
Figure 3.5. Schematic illustration of flocculation of silica and polymer chains.	34
Figure 3.6. Silica solubility test of Polyacrylamide (P1).....	35
Figure 3.7. The effect of Polyacrylamide (P1) on solubility of metal	36
Figure 3.8. Silica solubility test of Poly(acrylamide-co-diallyl dimethyl amonium chloride) (P3).	37
Figure 3.9. The effect of Poly (acrylamide-co-diallyl dimethyl amonium chloride) (P3) on solubility of metal.	38
Figure 3.10. Silica solubility test of Polyvinylpirrolidone (P4).....	39
Figure 3.11. The effect of Polyvinylpirrolidone (P4) on solubility of metal.....	40
Figure 3.12. Silica solubility test of Polyacrylic acid (P5).	41
Figure 3.13. The effect of Polyacrylic acid (P5) on solubility of metal.	42
Figure 3.14. The change on % transmission with concentration of HPAA.....	45

LIST OF TABLES

<u>Table</u>	<u>Page</u>
Table 2.1. The amounts of substances that is used for synthesis of artificial scale.....	21
Table 3.1. Elemental composition of natural and artificial scale / % concentration.	28
Table 3.2. ICP-MS analysis of decantate and EDX analysis of artificial silicates of parallel experiment's standart samples.	28
Table 3.3. Molecular structures of the inhibitors that was tested in this study.....	32
Table 3.4. Comparatively results of test of polymers at 20 ppm	33
Table 3.5. Solubility test of PVP on metals and silica.....	43
Table 3.6. Solubility test of PEG on metals and silica	43
Table 3.7. Solubility test of PAAMAA on metals and silica.....	44
Table 3.8. The effect of HPAA on metal concentration	45

CHAPTER 1

INTRODUCTION

1.1. Geothermal Energy and Scaling Problem

Geothermal energy is a thermal energy stored in form of heat under the earth's surface. It is reliable, sustainable, cost effective, and environmentally friendly energy source. Therefore, it has been widely used for many applications such as power generation, district heating system, chemical production, snow melting, fish industry and thermal tourism. However, geothermal brine can be extremely difficult to handle in geothermal operations. High temperature brine contains elements and compounds; however, causes operational limitations in geothermal power plants. These limitations are due to the severe scaling and corrosion of geothermal brine and steam (Figures 1.1.). Because of scaling, plants may have experienced extreme plugging in wells, lines and equipment. So, power plants face curtailment and even complete plant shutdown. Geothermal brine causes a variety of operational problems including equipment damage and failure, equipment repair and replacement, leaking and spilling of brine, well and line plugging, reduction of steam/brine flow, loss of power production and reduction of heat transfer effectiveness (Baba and Armonsson 2006).

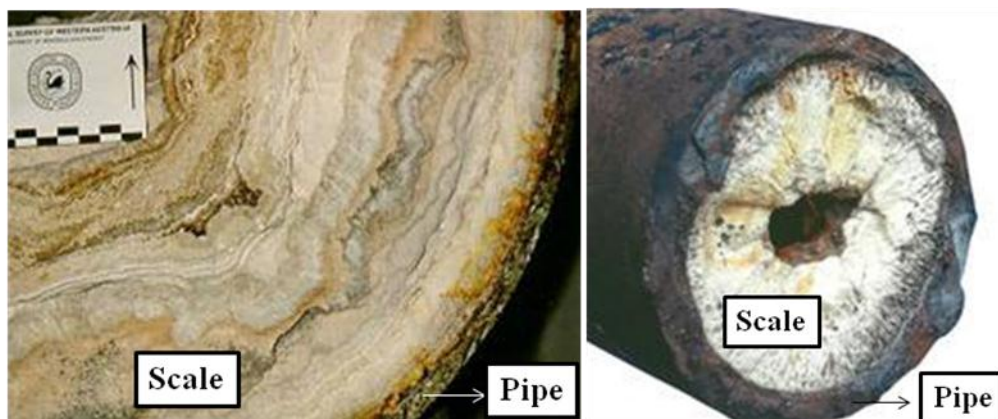


Figure 1.1. Scaling problem in some geothermal fields.
(Source: Doğan et al. 2013)

1.2.Types of Scaling

Different types of scales have been found in various geothermal areas. (Benevidez et al. 1988; Murray et al. 1995; Gunderson et al. 1995). The major species of scale in geothermal brine typically include calcium carbonate and silicate. As well as, some minerals can be seen such as calcium sulfate, calcium carbonate, barium sulfate, calcium oxalate and strontium sulfate scales and colloidal iron oxides (Zhang et al. 2011). Calcium compounds frequently encountered are calcium carbonate and calcium silicate. Metal silicate and metal sulfide scales are often observed in higher temperature resources. Typical metals associated with silicate and sulfide scales include zinc, iron, lead, magnesium, antimony, and cadmium.

1.3. Literature Review

1.3.1. Mechanism of Scaling

Exact mechanism of deposition is not clear but some approaches on how the process handle are available. Silicate is composed as a result of the polymerization of silica molecules (Figure 1.2). This polymerization is carried out in both acidic and basic environments. High amount of dissolved CO₂ is available in the underground hot water reserves due to high pressure. As brine flows through the well to the surface, the temperature of the brine decreases. As a result of decrease of pressure, CO₂ is released into the vapor phase. When the reservoir fluid loses its dissolved CO₂, pH of the brine increase and therefore the silica solubility decreases correspondingly. The brine phase becomes over saturated. At flash vessel, steam flashes and the temperature of the brine further decreases. The brine phase becomes more concentrated and the silica, already unstable, becomes even more unstable (Figure 1.3.).

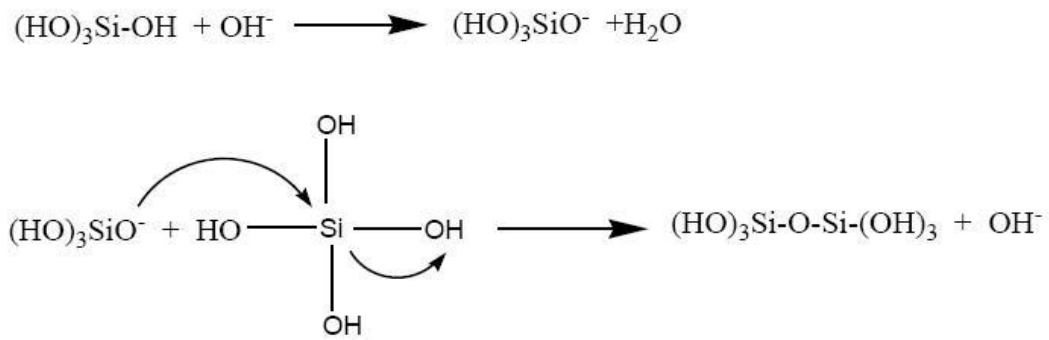


Figure 1.2. Polymerization reaction of ortho silicic acid.

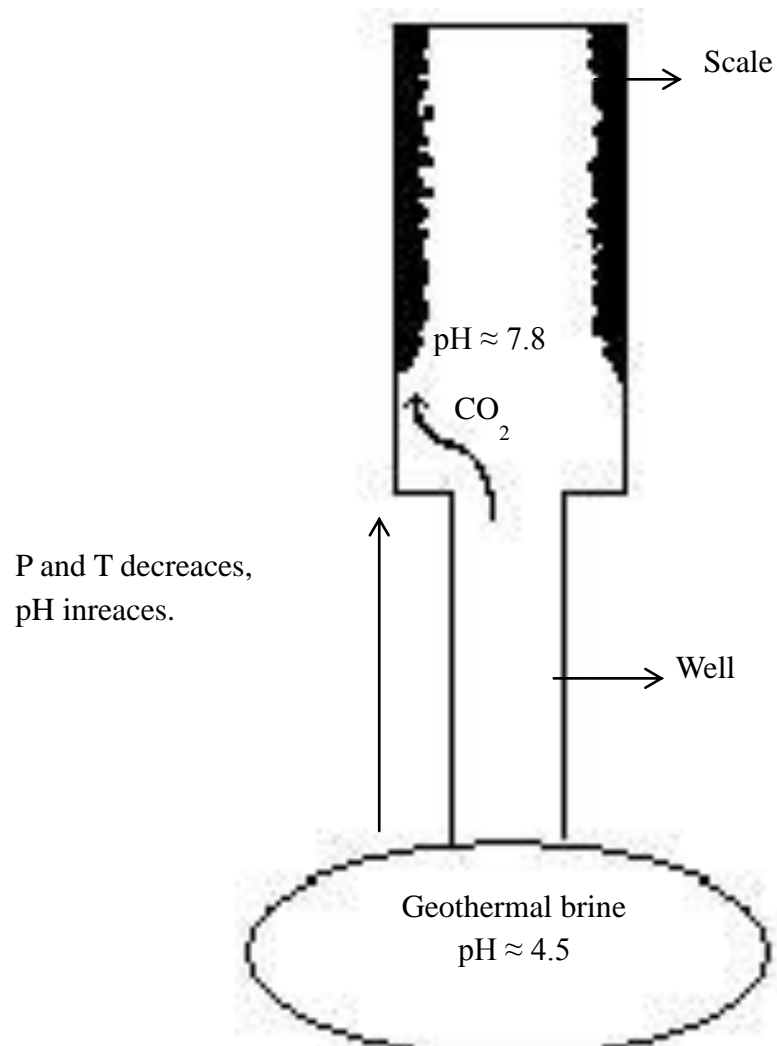


Figure 1.3. Schematic view of well.

Upon removal of CO₂, the pH of the water rises and the ions which are abundant in water such as Fe²⁺, Mg²⁺, Ca²⁺ precipitate as their hydroxides. pH also increases the percentage of silica polymerization simultaneously (Demadis 2010). Scale forms via condensation polymerization (Figure 1.2.). Metal hydroxide compounds interact with silica polymers and metal silicate compounds form which are harder to clean (Figure 1.4.). In addition to these ions such as Fe²⁺, Fe³⁺ and Al³⁺ which are effluent in the water from the worn pipe surfaces increases the silica deposition (Hayakawa et al. 1999). Formed silicate precipitate may be composed of numerous chains of different oligomeric structures just as in a polymer molecule of different molecular weights (Gallup et al. 2003). This silicate polymer has an amorphous form and similar to colloidal silica.

Polymerization of silica requires a balance of unionized and ionized silicate species. At higher pH, this balance is shifted towards the ionization of silicic acid and the polymerization of silica tends to slow down while the potential for the formation of metal silicates increases (Gill 1993). The reaction is catalyzed by hydroxide ions, so the reaction rate increases at pH 6.0-8.0. Above this pH range silicate species become important (Demadis et al. 2005).

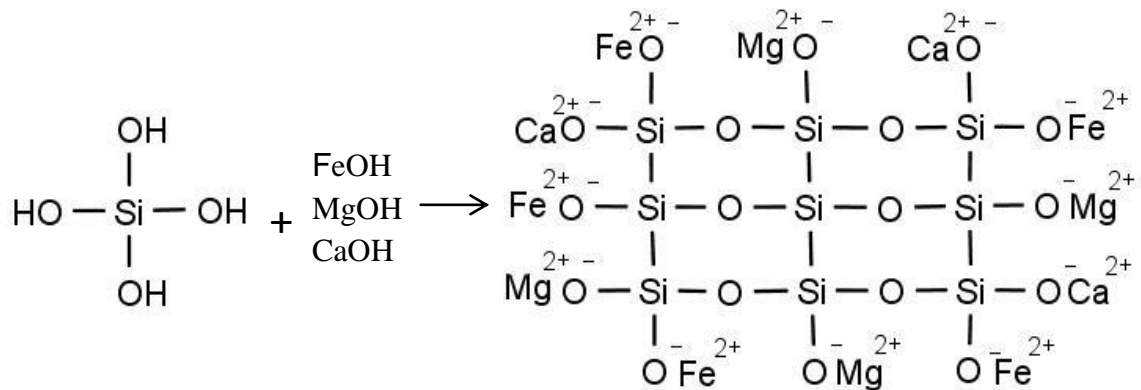
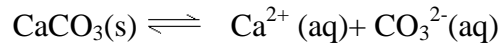
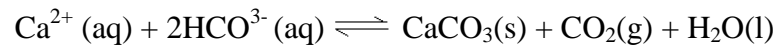


Figure 1.4. Schematic presentation of formation of metal-silicate particle.

Geothermal reservoir fluids are close to calcite saturation. It becomes more soluble when the temperature of the solution is high and when dissolved carbon dioxide (CO₂) is present in the solution. Degassing of such water, which occurs in response to boiling, leads to a sharp rise in the pH of water. This event in turn, causes the activity of the carbonate ion (CO₃²⁻) to increase significantly, leading to over-saturation (Arnórsson 1989).



Cooling, which occurs during depressurization and boiling, counteracts the effect of CO₂ degassing with respect to the state of calcite saturation (Arnórsson 1989). The release of CO₂ and deposition of calcite is conveniently expressed as:



Silica containing scale is arguably one of the most difficult scales occurring in geothermal operation. It is found virtually in all geothermal brine and its concentration is directly proportional to the temperature of the brine. This problem is being experienced at different power plants (Tarcán 2012) located in the various regions of the world (Gallup 1997) and it is one of the most controversial and researched issue. Indeed, some researchers who carry out studies on this subject, uses Gordian's Node which is the famous legend of Frigs as mythological metaphor in order to highlight the difficulties related to the solution of the problem (Demadis 2003). When we move this problem to a scientific reality aspect, we come across the fact that many studies have been conducted on this matter in the different regions of the world.

The methods that have been applied are mainly based on the principle of eliminating the silica deposition before it is formed. (Demadis et al. 2005; Stephalau et al. 2008). To prevent silica deposition, i.e. possible silicate polymerization, seems more advantageous for applications (Bergna 1994). However, there are no common solution path reported on this method due to the fact that silica deposition / accumulation mechanism yet not be fully resolved and geothermal waters show different characteristics in different regions (different salinity and temperature, etc.). In this respect, many researchers from various regions of the world offer different solutions.

Silicate formation is a quite complex mechanism and many factors should be taken into account while developing methods for it. Main approaches suggested for this purpose can be listed as low density process, prevention of other depositions, applying pretreatment and using inhibitors or dispersants. The newest approach among these methods is using blockers and dispersants; this method is preferred since the other methods did not take us to the desired efficiency. This method can be essentially summarized as reducing the reactivity of highly reactive silica molecules in the presence of metal hydroxide by using high weighted polymers that have polar groups, anionic groups or cationic groups and dendrimers. For instance, PAMAM dendrimers (Mavredaki et al. 2007), polyethylene imine (Stathouloupoulou et al. 2008), Inulin (Ketsetzi et al. 2008) can be used as preventer substances for silica polymerization. Dispersants may reduce the surface energy and prevent the incorporation of the particles by clinging on the surfaces of silica molecules/particles. This can reduce the effectiveness of the reactive silica with other molecules and convenient surfaces.

Formation of bulk scale includes some steps. At the beginning, colloidal silica particles form. When concentration and energy increase ions interact each other and nucleus forms. These small particles attach each other in order to decrease their surface energy. So, colloidal particles aggregate and then subsequently agglomerate. As a result bulk scale forms (Figure 1.5.).

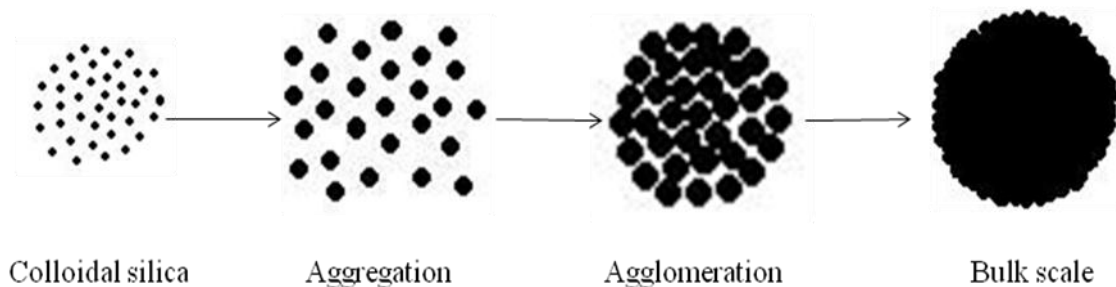


Figure 1.5. Tentative explanation for the formation of bulk scale.

1.3.2. Inhibitor Chemistry

To date, various molecules have been tried to inhibit the formation of silicate deposit. They are reviewed as below.

Dendrimers are repetitively branched globular molecules. They are called starburst polymers. Some dendrimers are effective silica inhibitors. For example, polyaminoamide (PAMAM). Schematic structure of PAMAM (Generation-1) and PAMAM (Generation-2) are shown in Figure 1.6. They can be COOH-terminated or NH₂-terminated.

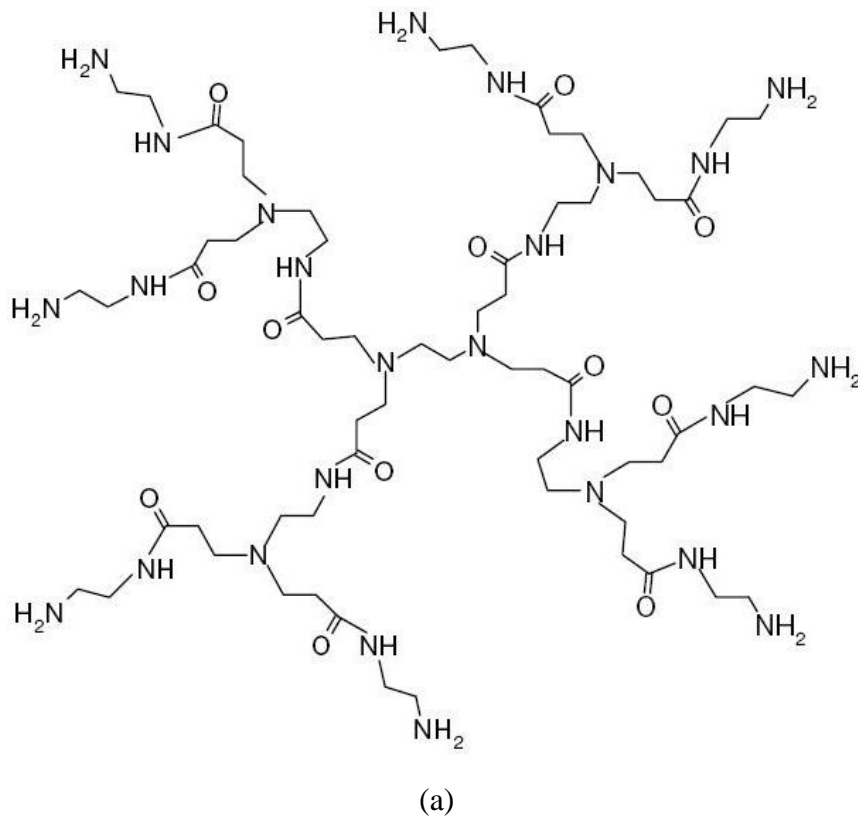
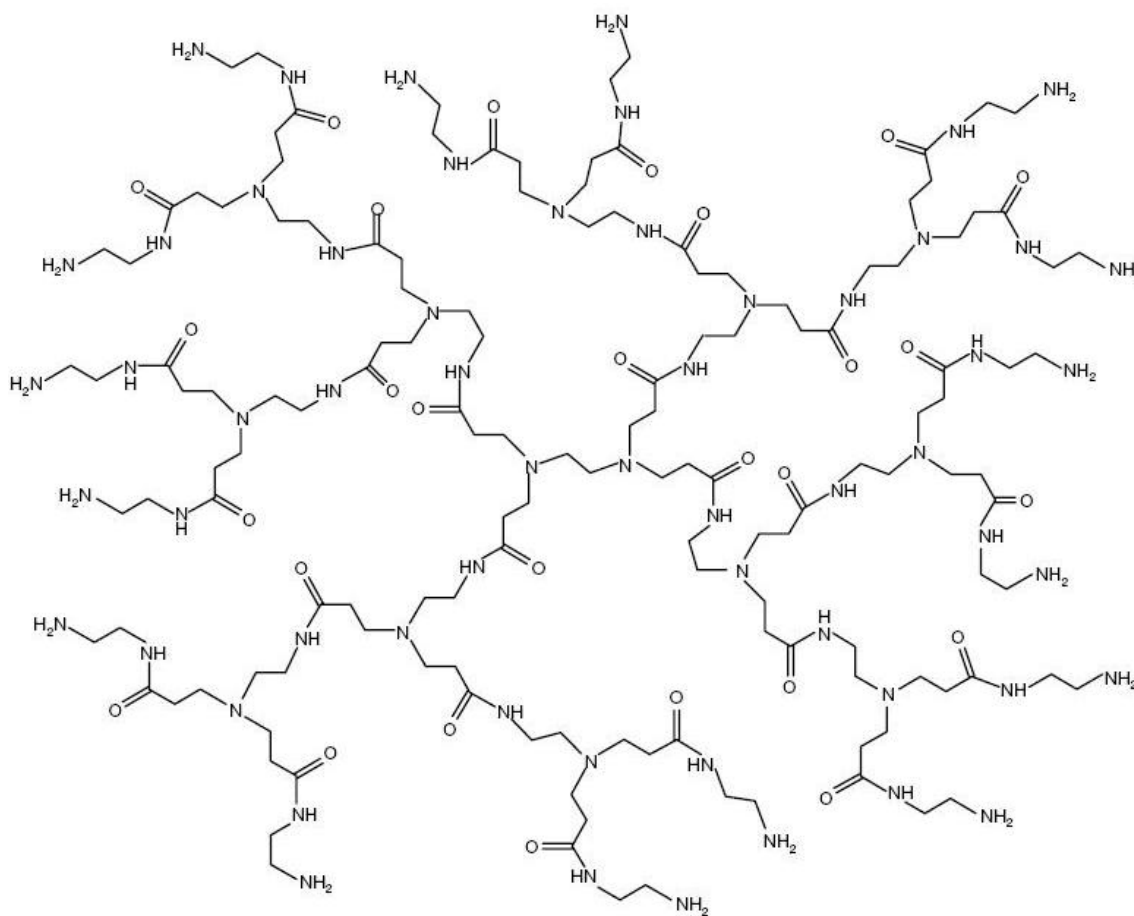


Figure 1.6. Molecular structure of (a) PAMAM (Generation-1) and (b) PAMAM (Generation-2) (Source: Demadis et al. 2007).

(Cont. on next page)



(b)

Figure 1.6. (Cont.)

Some studies were performed on inhibitor effectiveness of dendrimers. The result of effectiveness test of PAMAM-1 (Figure 1.7.), and PAMAM-2 (Figure 1.8.), is presented below (Demadis and Neofotistou 2004). Inhibitor effectiveness is a function of both concentration and time. PAMAM-1 and PAMAM-2 show similar features. At 20 ppm, inhibitors partially inhibit silica formation after 24 hours but for 48 and 72 hours SiO_2 values are indistinguishable. At 40 ppm, dramatic changes are observed for 24 hours (384 ppm SiO_2). After 48 and 72 hours, SiO_2 values decreases but still remains high (336 and 308 ppm SiO_2 , respectively). At higher inhibitor dosage, 60 ppm and 80 ppm, silica concentration values are decreases. General observation is that as time passes, silica levels drop and further increase on inhibitor dosage has adverse effect on its inhibiting ability.

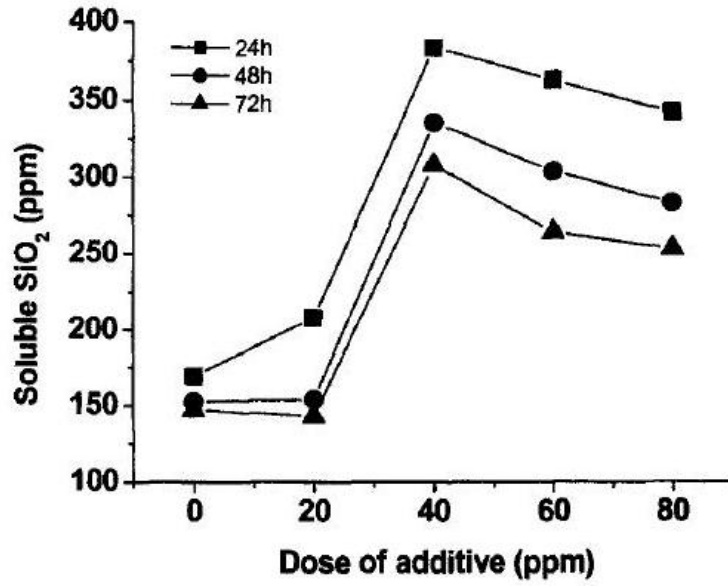


Figure 1.7. Solubility dependence of SiO₂ on PAMAM-1.0 dendrimer dosage.

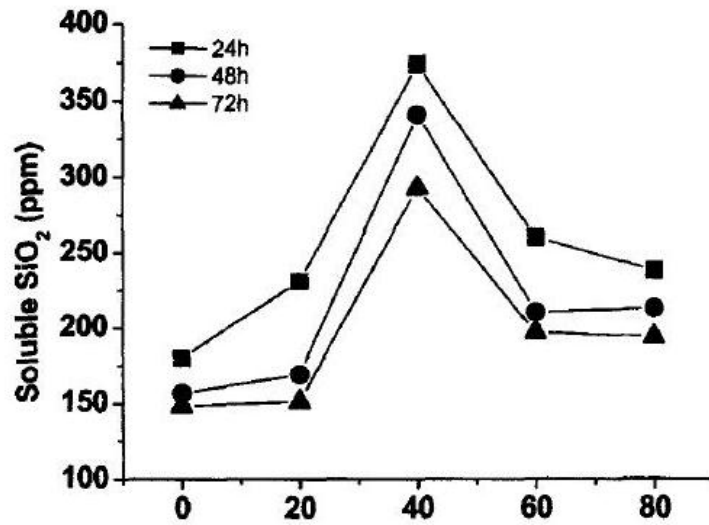


Figure 1.8. Solubility dependence of SiO₂ on PAMAM-2.0 dendrimer dosage.

Conventional mineral inhibitors are generally include phosphonic acid (Figure 1.9.) and carboxylic acid (Figure 1.10.). These chemicals have minimum influence on SiO₂ polymerization.

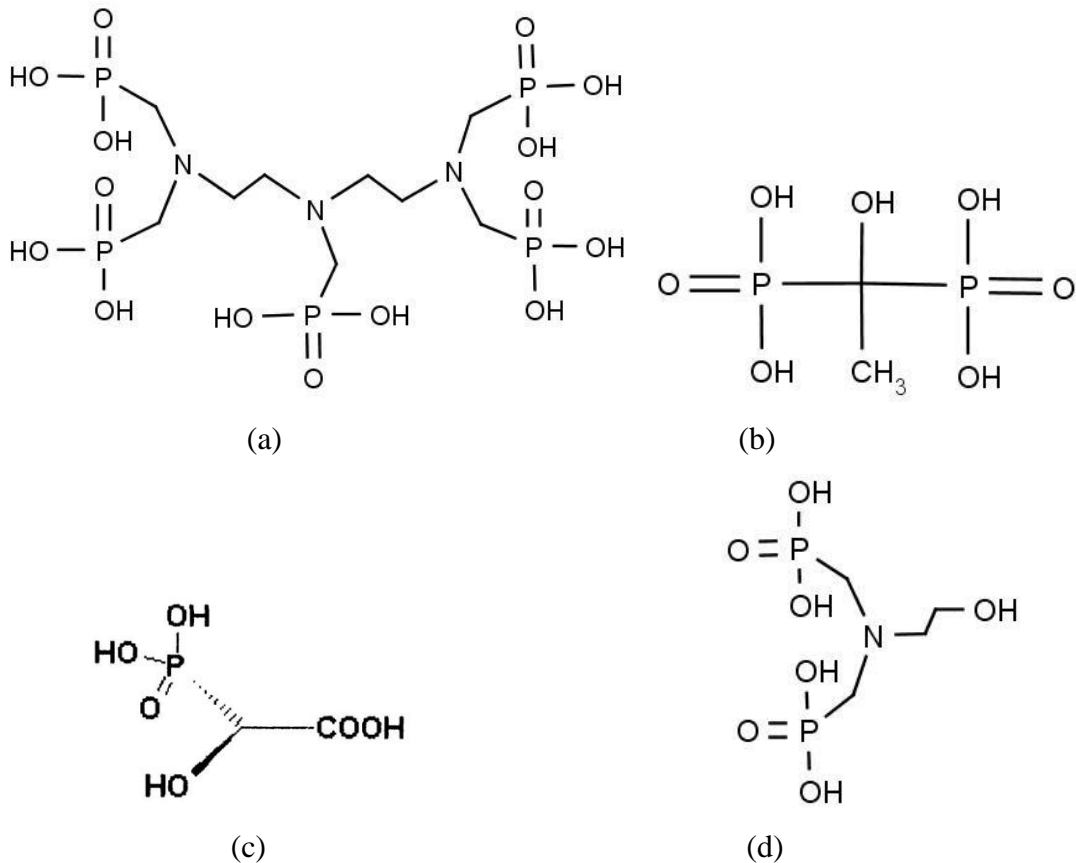


Figure 1.9. (a) Ethylene diamine tetra(methylenephosphonic acid), (b) 1-Hydroxyethyl diene-1,1-diphosphonic acid, (c) Hydroxy ethylene phosphono acetic acid, (d) Hidroxy ethylene amine phosphonic acid, (e) Hexamethylene-N,N',N',N'-diamine tetramethylenephosphonic acid, (f) Amino trimethylene phosphonic acid, (g) Amino-tris (methylenephosphonate) (Source : (a,b,c,d,e,f) Zhang et al. 2011 and (g) Demadis et al. 2007).

(Cont. on next page)

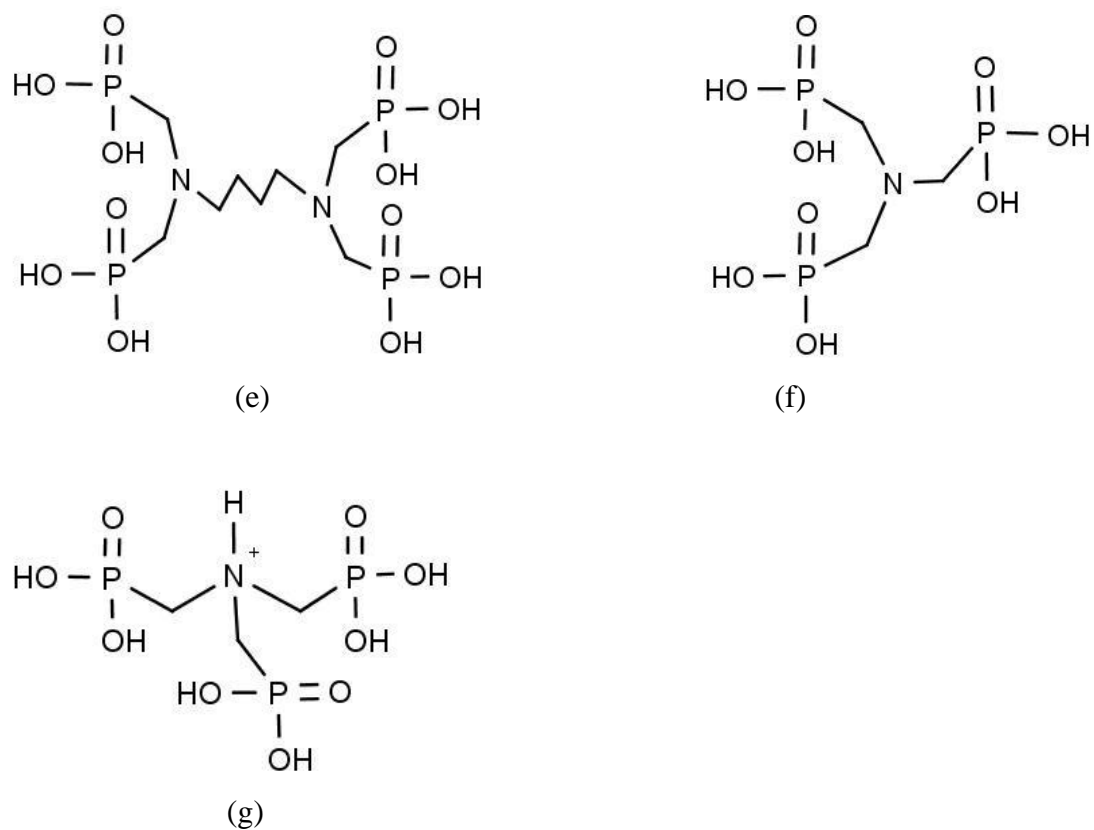


Figure 1.9. (Cont.)



Figure 1.10. (a) Polyacrylic acid, (b) Polymethacrylic acid, (c) Acrylic acid/methacrylic acid copolymer, (d) 2-phosphonobutane-1,2,4-tricarboxylic acid, (e) Carboxymethylinulin, (f) Polyethyloxazolin (AQUAZOL) (Source: (a,b,c) Zhang et al. 2011(d) Demadis et al. 2005, (e) Demadis et al. 2007, (f) Neofotistou et al. 2004).

(Cont. on next page)

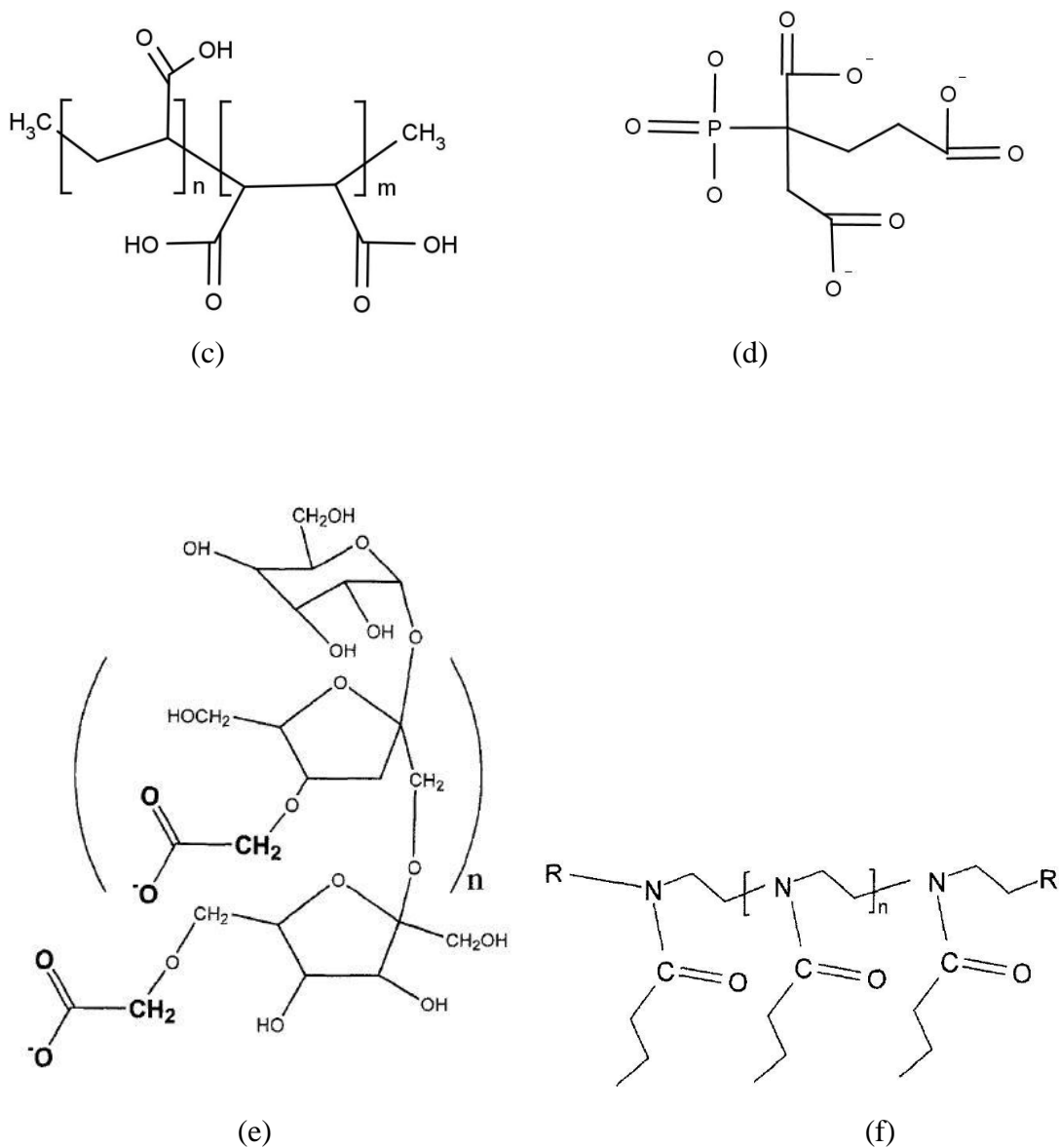


Figure 1.10. (Cont.)

The results of polyacrilate test in Figure 1.11. and 2-phosphonobutane-1,2,4-tricarboxylic acid in Figure 1.12. are given. According to these results, although they added at high concentration they don't have remarkable inhibitory efficiency.

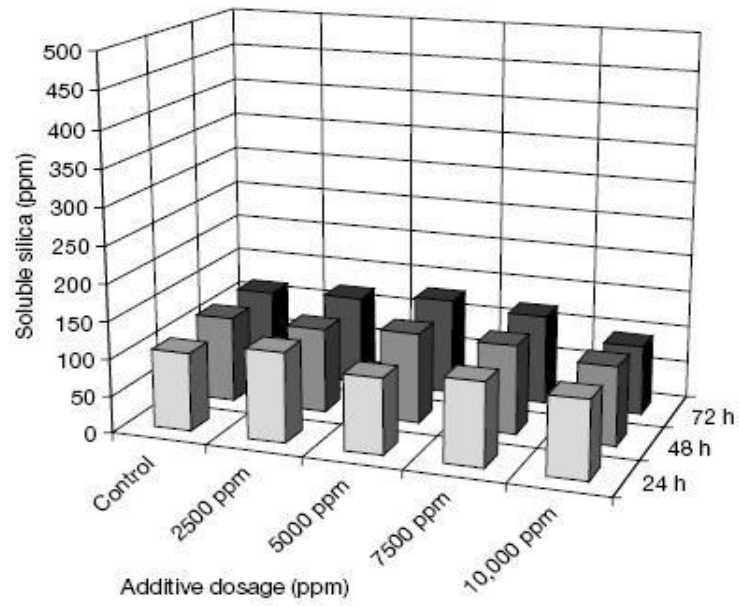


Figure 1.11. Effectiveness test of polyacrilate.
(Source: Demadis et al. 2007).

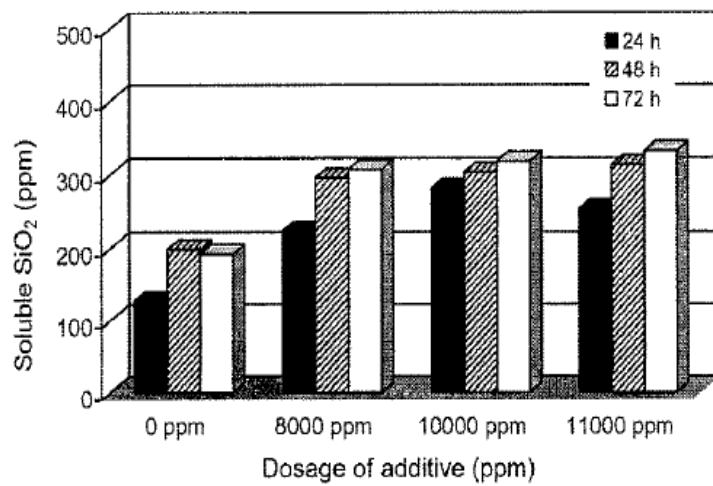


Figure 1.12. Effectiveness test of 2-phosphonobutane-1,2,4- tricarboxylic acid.
(Source: Demadis et al. 2005).

Some polymers that include amine or amide groups can also be used as scale inhibitor (Figure 1.13).

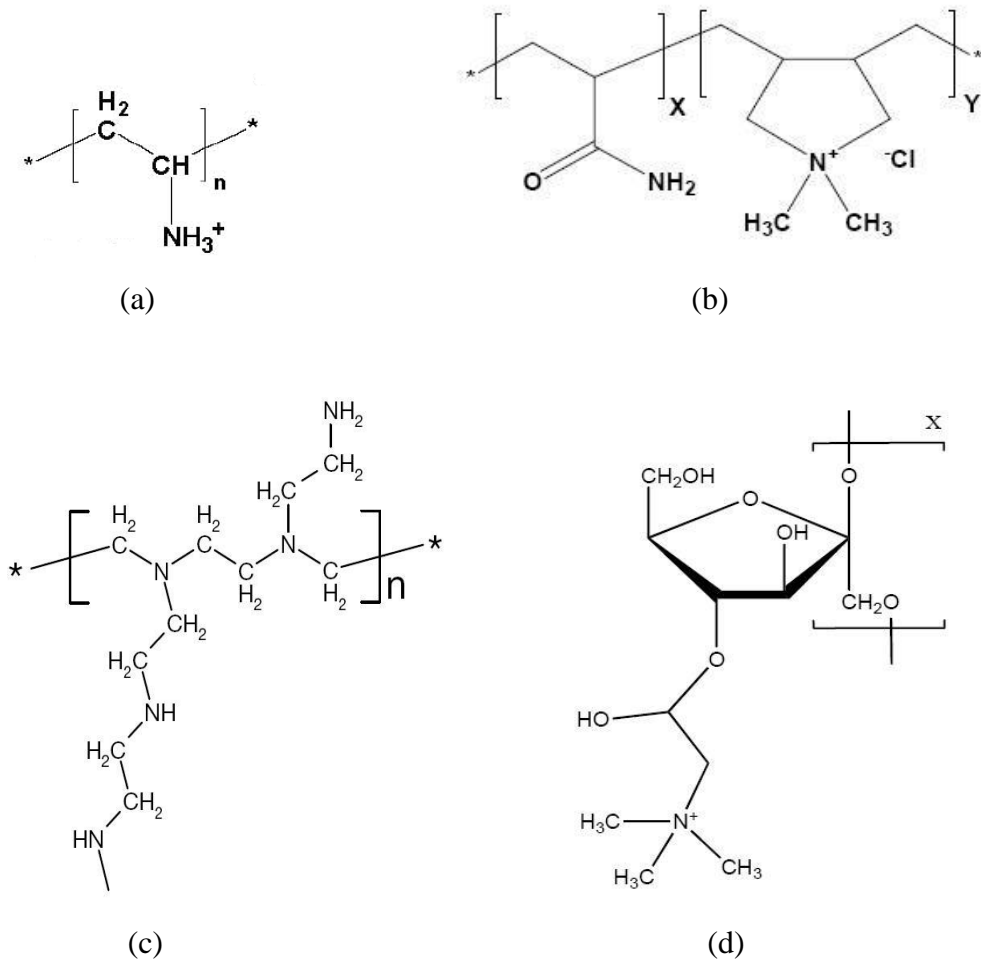


Figure 1.13. (a) PALAM, (b) PAMALAM, (c) Polyethyleneimin, (d) CATIN (Source : (a) Stathouloupoulou and Demadis 2008, (b) Ketsetzi et al. 2008, (c) Demadis 2007, (d) Ketsetzi et al. 2008).

Some studies were carried out on inhibitor effectiveness of inhibitors that include amine or amide groups. Results of test of some inhibitors that include amine or amide groups are given in Figure 1.14. and Figure 1.15. According to these results, although they are added at low concentration they exhibits high inhibitor efficiency in short time. In Figure 1.14., 20 ppm PALAM was added, as a result, it is seen approximately 150 ppm increase at soluble silica concentration. In Figure 1.15., 80 ppm CATIN and PAMALAM were added. After reaction, approximately 200 ppm increase is seen at soluble silica concentration.

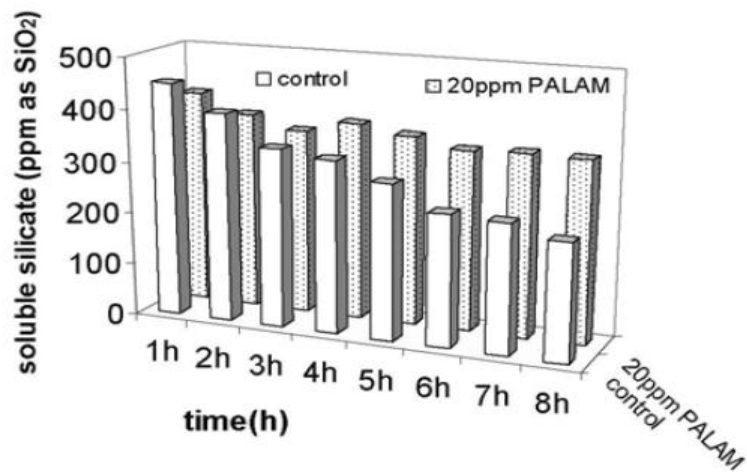


Figure 1.14. Solubility test of silicate in presence of 20 ppm PALAM. (Source: Stathouloupoulou and Demadis 2008).

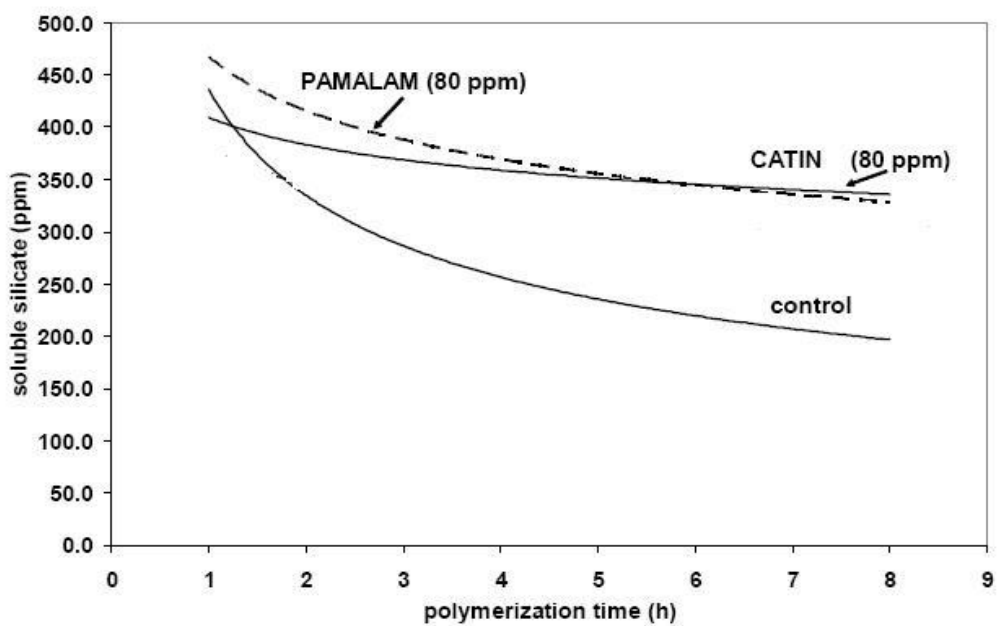


Figure 1.15. Solubility test of silicate in the presence of PALAM and CATIN. (Source: Ketsetzi et al. 2008)

In Figure 1.16., the result of effectiveness test of polyethylene imine is presented. Inhibitor effectiveness is a function of both concentration and time. Polyethylene imine is more effective at 10 ppm and 24 hours. Because at higher concentration polyethylene imine attach to silica molecules and precipitates (Demadis et al. 2007). At 48 hours and 72 hours soluble silica concentration decreases. Since polyethylene imine just retards the reaction.

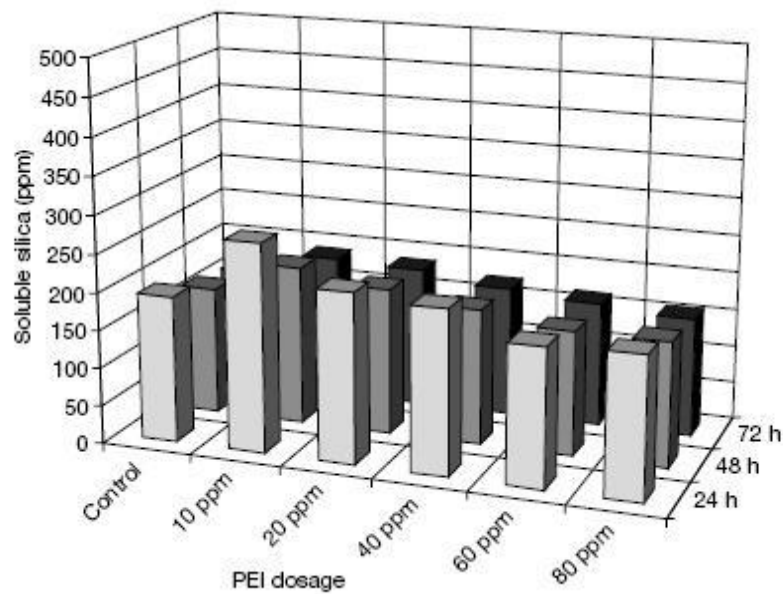


Figure 1.16. Effectiveness test of polyethyleneimine.

Different approaches have been developed and solutions have been searched to understand and solve the deposition of silica. Earlier studies have been made in different fields to find a silicate indicator.

1.4. Aim of the Study

Scaling is an important problem in almost all geothermal fields. Even though there are many studies being carried out to minimize scaling using inhibitors, existing inhibitors do not run effectively. The aim of the study is to test the efficiency of potential inhibitors including commercial ones and as well as macromolecules that may act as inhibitor. First, we focused on the fabrication of synthetic scale. This methodology is considered as key step for testing the efficiency of inhibitors employed. For this aim, the structure of the scale formed in the geothermal fields will be analyzed to gain a better understanding of its formation. Then, the effectiveness of the substances which may act on the metal-silicate compounds is tested.

The natural scale samples are obtained from Tuzla GEP Co. Since Tuzla has highly saline water and several metal-silicate forms in their pipelines (Doğan et al. 2013). Tuzla GEP Co. locates northern-west of Turkey, 80 km south of the city of Çanakkale, in Tuzla (Figure 1.17.).

Tuzla is an active geothermal area hosted by rhyolite lava and pyroclastic deposits. Geothermal brine is found in a shallow volcanic reservoir at a depth of between 330 m to 550 m and a deep marble reservoir can be seen at depth of 530 m. TGF is an interesting area in Turkey from the point of its temperature and dissolved ions in the water. The chloride concentration of Tuzla geothermal brine reaches 68 256 mg/L, which is nearly twice the concentration of seawater and is termed “brine” water.

In the Tuzla area, the origin and nature of the thermal springs have been investigated by Mützenberg (1997). Tuzla geothermal field’s environmental properties were described by Baba (2003), Baba and Özcan (2004), and Baba et al. (2005). It was found that the Tuzla hot brine has a high tendency to scaling (Tarcan 2005). According to previous resources, Tuzla geothermal brine forms as a result of the dissolution of marine evaporates and chemical alteration (dissolution of halite, dolomitization, reduction of sulphate, precipitation of anhydrite, diagenetic reactions of silicates, Ca and Na ion exchange and reactions with organic matter). These alteration generates the higher mineralization. There are alternate models for the origin of the TGF that include derivation from relics of evaporated seawater trapped in sediments, dissolution of Messinian evaporites and trapped relict seawater within pore spaces in rocks (Baba 2009).

CHAPTER 2

EXPERIMENTAL SECTION

2.1. Chemicals and Reagents

Troughout this study Poly(vinyl sulfate, potassium salt) (Aldrich), Polyacrylamide (Aldrich, 50 wt. % solution in water), Calcium chloride dihydrate (Sigma- Aldrich, $\geq 99.0\%$), Sodium carbonate (Sigma- Aldrich, 99.0 %), Magnesium chloride hexahydrate (Emsure, for analysis), Iron(II)chloride tetrahydrate (Sigma- Aldrich, 99.0 %), Oxalic acid dihydrate (Emsure, extra pure), Ammonium heptamolibdate tetrahydrate (Emsure, extra pure), Sodium silicate (Emsure, % 27 SiO₂ containing water solution), NaHCO₃ (Sigma, 99.5 %), NaCO₃ (Sigma, 99 %), Poly(acrylic acid) (Aldrich, M_w 1,800), Poly(acrylamide-co-diallyl dimethyl amonium chloride) (Aldrich, 10 wt. % in water), Polyvinylpyrrolidone (Alfa Easer, M_w 8,000; Fluka, M_w 10,000; M_w 40,000 and Aldrich M_w 55,000), Polyethylene glycol (Alfa Easer, M_w 2,000 and Emsure, M_w 6,000), Polyacrylamide-co-acrylic acid (Aldrich, M_w 200,000 and Aldrich, M_w 5,000,000) were used without further purification or process. All solutions were prepared with ultra pure water.

2.2. Sampling and Characterization of Natural Silicate

Natural silicious scale was observed at different locations in Tuzla geothermal system. There are many units in the system such as wellhead, pipeline, separator, vaporizer, preheater, and re-injection well. Since scale in the vaporizer is problematic for the system. Natural scale was obtained from vaporizer for analyses and reference for artificial scale fabricated in our lab. Both natural and synthetic scales were characterized in terms of elemental composition, crystal structure, and morphology.

2.3. Synthesis of Artificial Silicate

A solution was prepared by using the below listed salts (Table 2.1.) so as to synthesize artificial silicate identically. This solution was heated to 90 °C by reflux for four hours. (Figure 2.1)

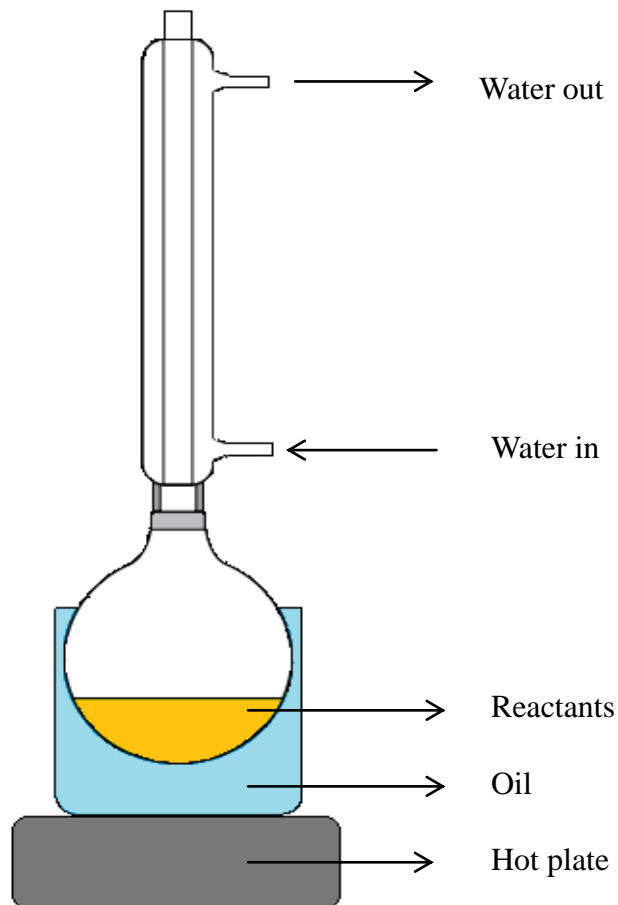


Figure 2.1. Schematic illustration of reflux.

Since the study is focused on the efficiency of inhibitors for the formation of Fe-Mg-Ca-Silicate, Fe, Mg ve Ca salts were employed for the fabrication of silicate. Metal silicate synthesis is obtained by using $\text{FeCl}_2 \cdot 4\text{H}_2\text{O}$, $\text{MgCl}_2 \cdot 6\text{H}_2\text{O}$, $\text{CaCl}_2 \cdot 2\text{H}_2\text{O}$ and NaCO_3 salts have been used which are water soluble salts. Salt solutions ratios relative to each other were arranged as per the elemental compositions of silicates gained as a result of the trials.

Table 2.1. The amounts of substances that is used for synthesis of artificial scale.

Reactive	Amount (mg/L)
MgCl ₂ .6H ₂ O	508
FeCl ₂ .4H ₂ O	284
CaCl ₂ .2H ₂ O	14
NaCO ₃	10
Sodium silicate	3000

In addition to these salts, aqueous Na-silicate solution containing 27% of SiO₂ was added. It was added as 3g SiO₂ / L. Teflon covered magnetic stirrer was placed in the flasks and stirred in the reflux assembly; it was left for 4 hours at 90 °C (Figure 2.2.).

Afterwards, the heaters were closed and the mixture in the flasks was left for 1 hour to cool down and for the crystal formation. Silicate mixture was separated by centrifugation (6000 rpm, 30 min). Silicate was left at 90 °C overnight so as to crystallize and dry scale. Finally, elemental and morphological analysis was performed for characterization.

For the determination of ion concentrations remaining in the decantate, the Inductively Coupled Plasma-Mass Spectrometry and Visible and Ultraviolet Spectroscopy analysis was performed.

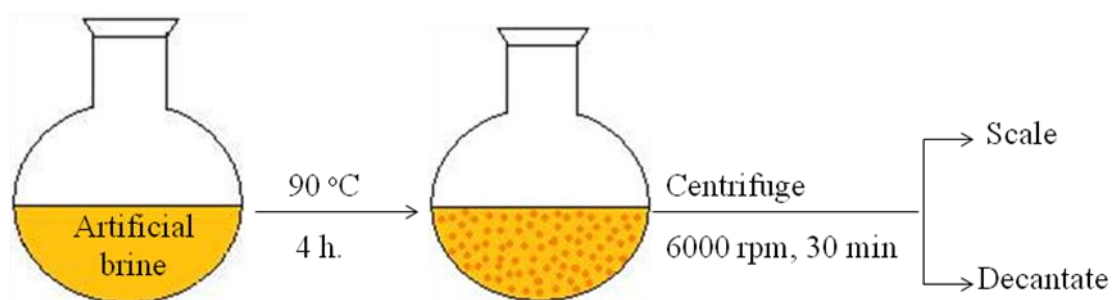


Figure 2.2. Schematic view of procedure for the formation of synthetic scale.

2.4. Inhibitor Tests

Some potential polymeric inhibitors were chosen that is water soluble and commercially available. Inhibitors were added into the artificial brine media to test the effectiveness of the inhibitors. Different inhibitors and their effectiveness at different concentrations were studied. In addition, at different time effectiveness of inhibitors were tested.

UV-Visible spectrometry and spectrophotometric method using silicomolibdate was applied on the decantate, which is obtained after the synthesis carried out with inhibitor substances to determine the concentration of suspended silica. The suspended silica concentration increases with the inhibitor effectiveness. The better inhibition, the higher the concentration is. As a result of interaction between silica and inhibitors, reaction rate decreases.

The inhibitor effectiveness was compared based on the concentrations of metal ions as reference, which do not react with silica due to their interaction with inhibitors. Chromatography and spectroscopy analyses were made to determine the concentration of suspended Fe^{2+} , Mg^{2+} and Ca^{2+} .

2.5. Characterization Tools and Applied Methods

The characterization of scale and determination of metal cations concentrations in addition to concentration of silica in the liquid phase were performed using the techniques in the following sections.

2.5.1. Scanning Electron Microscopy (SEM)

Scanning electron microscope (SEM) uses accelerated electrons as probe instead of photon in light microscope to obtain image. It provides higher resolution compared to light microscope. The electrons interact with atoms in the sample, producing various signals that contain information about the sample's surface. One can analyse both morphology and elemental composition by SEM. Image analysis was

performed by using a FEI Quanta250 FEG type instrument at IZTECH-Center for Materials Research.

The powder samples were sprinkled onto C tapes which are adhesive and supported on metallic disks. In order to provide electric conductivity the silica surface is coated with gold. Morphological properties of the sample surfaces were analyzed using Back Scattered Electron detector.

2.5.2. X-ray Diffractometry (XRD)

X-ray Diffractometry (XRD) is an analytical technique that provides information about the various forms of phases and crystals in the structure of the solid or powder sample. This technique provides information about phases that contain in a material, the concentration of this phases, the amount of non-crystalline phase and crystal size. XRD analyses were carried out by Philips X'Pert Pro diffractometer at IZTECH-Center for Materials Research. After reaction, the deposit is separated by centrifugation and dried at furnace. Solid samples were grinded using mortar and putted on the sample holder by adhesive. The analysis were performed with 2Θ range of 5° to 80° .

2.5.3. X-ray Fluorescence (XRF)

XRF spectroscopy is the technique of analyzing the fluorescent X-Rays in order to gain information about the elemental composition of a particular material. Solid samples were grinded using mortar. XRF analyses were carried out by Spectro IQ II at IZTECH-Center for Materials Research.

2.5.4. Inductively Coupled Plasma Mass Spectrometry

Inductively coupled plasma mass spectrometry (ICP-MS) is a type of mass spectrometry which is capable of detecting metals and several non-metals. ICP-MS is an efficient and highly sensitive tool. It can analyse samples from low parts-per-trillion (ppt), up to parts-per-billion (ppm). The plasma with it's high ion density and high temperature provides a good atomizer and ionizer.

After centrifuge % 2 HNO₃ was added to samples and kept in refrigerator. Analysis were performed by AGILENT 7500ce at IZTECH Environmental Development Application and Research Center.

2.5.5. Zeta Sizer

Zeta sizer is a technique that is used to determine the size of various particles including proteins, polymers, micelles, carbohydrates and nanoparticles, electrophoretic mobility of proteins, zeta potential of nanoparticles and surfaces, and optionally the microrheology of protein. The exceptional performance also enables the measurement of the molecular weight. The measurement depends on the size of the particle, the surface area, particle concentration, and the type of ions. Samples measured after and before centrifuge. Samples were put in pet cuvette with length 1 cm. Analysis were performed by Malvern Zetasizer Nano-ZS. The Zetasizer Nano ZSP has highest sensitivity for size and zeta potential measurement.

2.5.6. Visible and Ultraviolet Spectroscopy

Ultraviolet-visible spectroscopy method depends on absorption spectroscopy or reflectance spectroscopy in the ultraviolet-visible region. In absorption it measures the intensity change of light passing through the sample. When light passes through or is reflected by a sample, a characteristic portion of the mixed wavelength is absorbed. The absorption or reflection associated with the concentration of the sample.

Silicomolibdate spectrophotometric method was used. Liquid sample was put in quartz cuvette. Absorbance was measured at 410 nm. UV analysis was performed by using a Shimadzu W-2550.

2.5.7. Silicomolibdate Spectrophotometric Method

Silicomolibdate spectrophotometric method was used in order to analyze suspended silica concentration. We can measure soluble silica concentration by using this method,

not only monomers but also dimers, trimers, tetramers, etc. Soluble or reactive silica donates soluble silicic acid.

First of all, samples and standards are prepared. After reaction, decantate is centrifuged and without add acid is kepted at refrigerator. Because acid leads to precipitation of silica. Samples can be kepted for 28 days in this condition. For all sample, blank solutions are prepared. So as to plot calibration curve standard solutions are prepared. Main standard silica solution is prepared. 4.73 g sodium meta silicate nanohidrate ($\text{Na}_2\text{SiO}_3 \cdot 9\text{H}_2\text{O}$) is solved in 1000 mL water (Main solution (1000 ppm)). Later, 0 ppm, 1 ppm, 5 ppm, 10 ppm, 15 ppm, 25 ppm, 50 ppm standard solutions are prepared. Than, in order to convert unreactive silica to reactive silica, 200 mg solid NaHCO_3 is added for 50 mL solution of samles, blanks and standart. After addition of NaHCO_3 , solutions are waited at hot water bath for 1 hour and are cooled. Than, so as to decrease pH, H_2SO_4 and HCl is added. 27.6 mL H_2SO_4 is putted in flask and completed to 1 L. 1+1 HCl is used. 500 mL HCl is diluted to 1 L. 2.4 mL H_2SO_4 and 2 mL 1+1 HCl solution are added to all samples, blanks and standards. And than, ammonium molybdate was added. 10 g Ammonium hepta molibdate tetra hidrate ($(\text{NH}_4)_6\text{Mo}_7\text{O}_{24} \cdot 4\text{H}_2\text{O}$) is solved in 100 mL ultra pure water. pH of Ammonium molybdate salotion is adjusted to 7-8 by using HCl and NaOH. 2 mL Ammonium molybdate solution is added to samples and standartds and waited for 10 minute (It's not added to blanks). Finally, oxalic acid is added. 7.5 g oxalik acit ($\text{H}_2\text{C}_2\text{O}_4 \cdot \text{H}_2\text{O}$) is solved in 100 mL ultra pure water. 2 mL Oxalic acid solution is added to all samples, blanks and standards. After 2 minutes and measured at 410 nm, with light path 1 cm. At first, standards are measured and calibration curve is obtained.

For baseline, 0 ppm standart is used. The detectable concentrations range is 0-75.0 pmm. The appropriate dilution factor is applied in order to calculate the samples concentration.

The silicomolibdate method is based on reaction of ammonium molibdate with silica and phosphates. As a result of this reaction, the color of solution turns out to yellow. In order to destroy molybdophosphoric acid, oxalic acid is added. Thus, the interference of molybdophosphoric acid with silicomolybdate is prevented (Neofotistou and Demadis, 2004).

CHAPTER 3

RESULTS AND DISCUSSIONS

3.1. Identification of Natural Scale

Natural scale was obtained from Tuzla region and subjected to chemical and structural analysis. The results suggest that the deposit has amorphous like (Fe,Mg) silicate structure. However, the stoichiometric composition was varied. In order to find an effective inhibitor chemistry for scaling problem, synthetic scale was prepared in the laboratory to have a serial trials to have similar composition and structure. Their comparison will be given in the following section.

3.2. Fabrication of Synthetic Scale

The recipe for the fabrication of synthetic scale is developed based on the elemental and structural composition of natural scale. The scale obtained from Tuzla region is analyzed and realized that it is (Fe,Mg) silicate with very low crystallinity. The artificial scale obtained from reflux of synthetic brine was subjected identical analyses.

Figure 3.1. presents SEM images of both natural (left panel) and artificial (right panel) silicious scale. Both images show amorphous colloidal silica with submicro diameter. Figure 3.2 illustrates X-ray diffraction profiles of both deposits. They have low intensity reflections at almost the same angles. A search match analysis suggests that the diffractogram shows Saponite/Hectorite like amorphous structures and contain Fe-Mg-Ca silicates. The elemental compositions of the scales were determined by XRF. The results are given in Table 3.1. The deposits are mainly composed of Fe, Mg, Ca, and Na. Based on these results, one can claim that the artificial deposit has similar, structural, morphological, and elemental composition with natural one.

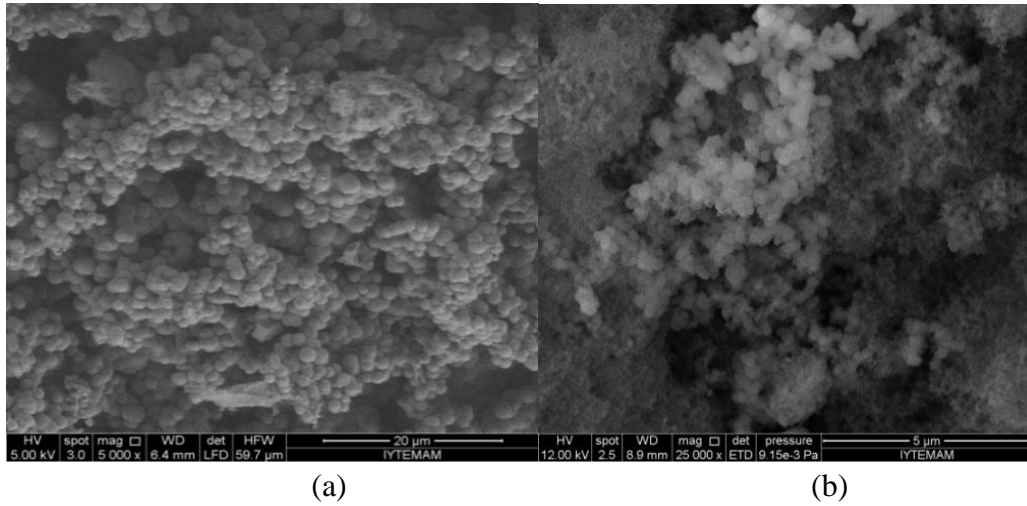


Figure 3.1. Morphological features of (a) natural scale and (b) artificial scale.

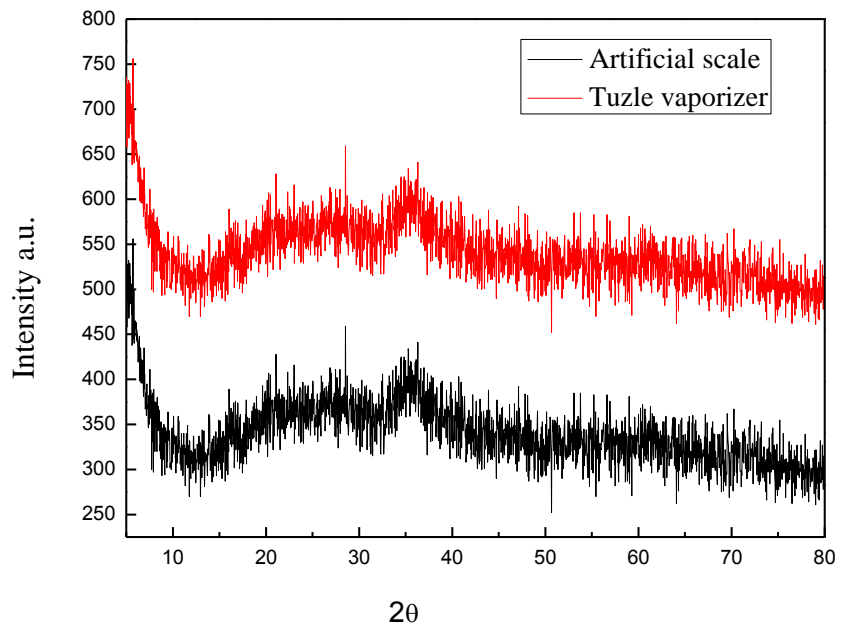


Figure 3.2. XRD patterns of natural scale and artificial scale.

Table 3.1. Elemental composition of natural and artificial scale / % concentration.

Element	Natural scale	Artificial Scale
O	62.76	63.27
Na	1.38	0.00
Mg	5.03	3.83
Si	9.86	13.56
Cl	0.70	0.00
Ca	0.40	0.35
Fe	2.42	6.00

The fabrication of artificial silicate is performed in a reaction solution given in Experimental Section. A synthetic brine is refluxed for overnight and artificial deposit is precipitated. The deposit is isolated from the reaction mixture by centrifugation. The decantate of the mixture is subjected to elemental compositions. Table 3.2. shows the concentrations of metal cations in decantate solution. The experiment has been performed three times this is because the results are given in a standard error. Thus, the results has high precision and approach we employed for fabrication of deposit is robust.

Table 3.2. ICP-MS analysis of decantate and EDX analysis of artificial silicates of parallel experiment's standard samples.

Ion	Decantate / ppm
Fe ²⁺	23.1 ± 0.4
Mg ²⁺	18.4 ± 0.4
Ca ²⁺	2.0 ± 0.1
Si ⁴⁺	-

The reaction mixture was analyzed by UV spectroscopy. The idea for the analysis was to validate the formation deposit indirectly. Three measurement was performed for salt solution without refluxing, salt+ Na-Silicate solution before reaction, and decantate after refluxing. Figure 3.3. shows % transmission of reaction mixture over visible range of optical spectrum. The transmission of reaction mixture decreases compared to both standard and salt solution. This decrease can be attributed to formation of silica colloids, which is considered as the building block of the deposit. The size of the colloids comparable with visible light and causes optical scattering. Scattering of colloids may reduce the percent transmission.

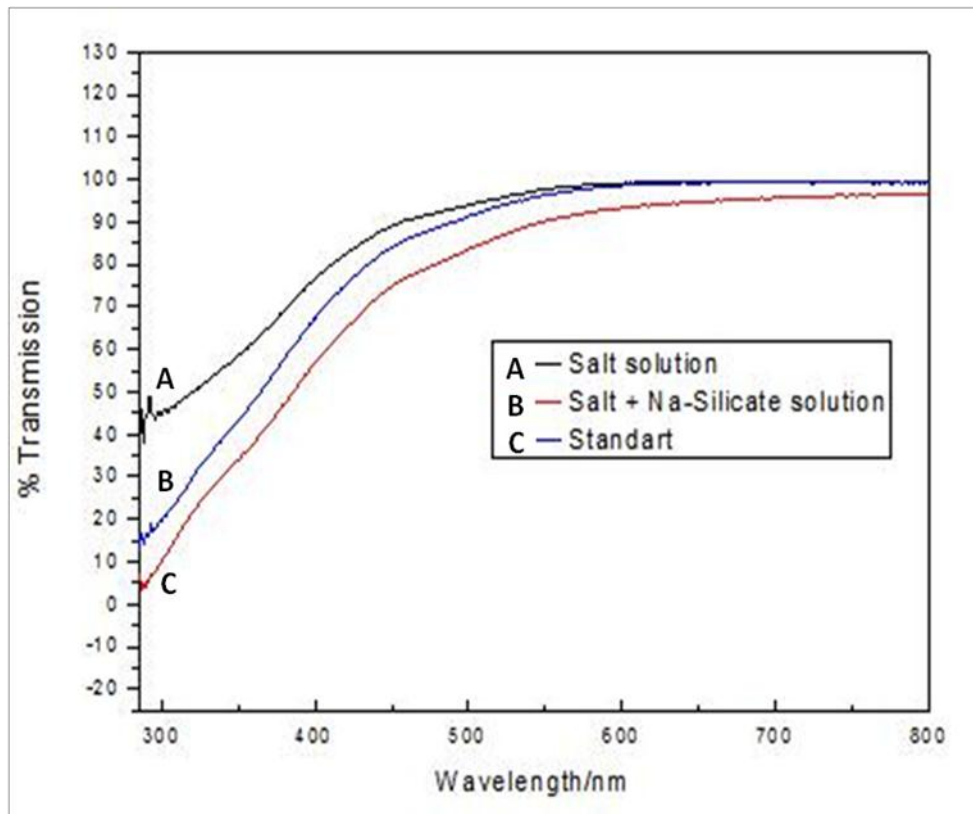


Figure 3.3. UV results of change that observe during preparation sample while Fe-Mg-Ca Silicate synthesis. (A) Just salt solution, (B) salt+Na-Silicate solution before reaction, (C) decantate after reaction.

After silicate formation reaction by refluxing the synthetic brine overnight, the reaction mixture was characterized by Dynamic Light Scattering before and after centrifugation. Prior to centrifugation there are two population of particles centered at 20 nm and 110 nm (panel A of Figure 3.4.). After centrifugation process, the size is reduced to 20 nm. This result indicates that the centrifugation condition (1 h, 6000 rpm) is enough to precipitate the colloids with a size of 110 nm; however, not enough for the precipitation of smaller particles. This result supports the result given in Fig. 3.3. indicating the formation of colloids in reaction mixture.

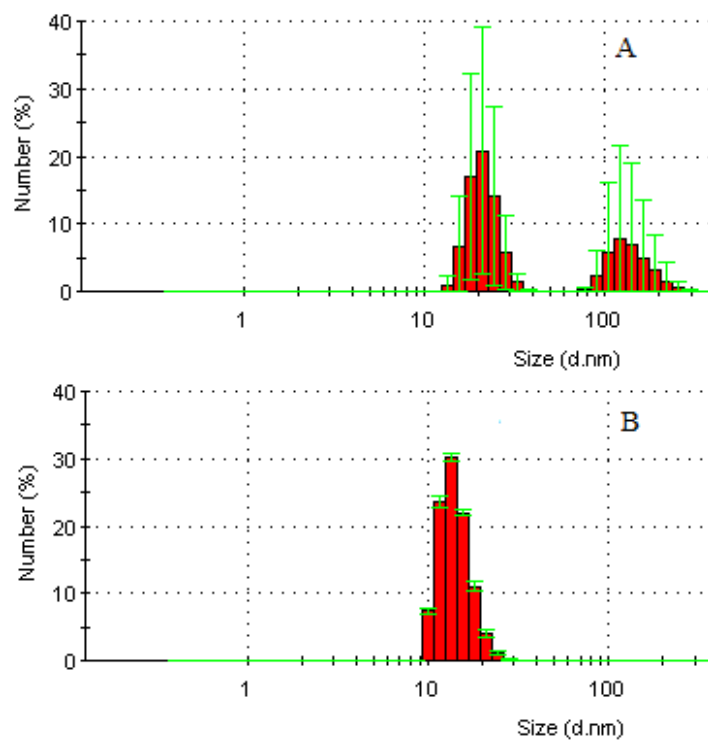


Figure 3.4. (A) Before centrifuge and (B) after centrifuge.

3.3. Inhibition of Scale by Polymeric Compounds

In addition to commercial inhibitors, there are polymeric molecules that may act as inhibitor for silicious deposits. Testing of the inhibitors in real geothermal system is costly in terms of time and budget wise. In this section, some water soluble polymers (Table 3.3.) containing amide, sulfate, carboxyl groups were tested in controlled laboratory conditions (20 ppm, 5 h).

Comparatively results of test of polymers at 20 ppm are given below (Table 3.4.). The results of solubility of metals in presence of polymers do not show pronounced difference. Because inhibitor concentration is not so high. On the other hand, differentiation in Si concentration is clear. According to these results polyacrylamide is the most effective polymer at 20 ppm.

Table 3.3. Molecular structures of the inhibitors that was tested in this study.

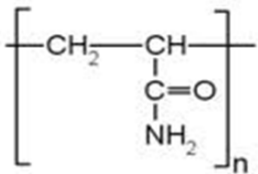
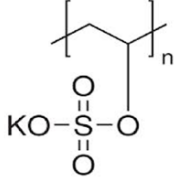
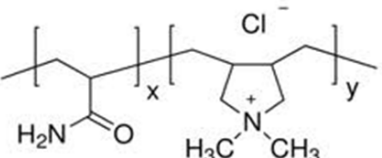
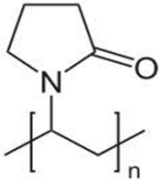
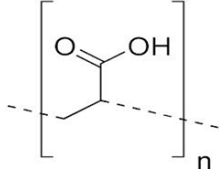
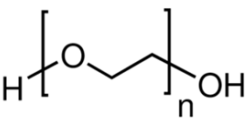
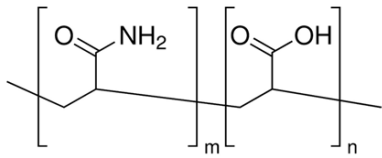
<p style="text-align: center;">P1 Polyacrylamide</p> 	<p style="text-align: center;">P2 Poly (vinyl sulfate, Potassium salt)</p> 
<p style="text-align: center;">P3 Poly(acrylamide-co-diallyl dimethyl amonium chloride)</p> 	<p style="text-align: center;">P4 Polyvinylpyrrolidone</p> 
<p style="text-align: center;">P5 Polyacrylic acid</p> 	<p style="text-align: center;">P6 Polyethyleneglycol</p> 
<p style="text-align: center;">P7 Poly(acrylamide-co-acrylic acid)</p> 	

Table 3.4. Comparatively results of test of polymers at 20 ppm. (All units are given in terms of ppm.)

	[Mg ²⁺]	[Ca ²⁺]	[Fe ²⁺]	[ΣM ⁿ⁺]	[Si ⁴⁺]
Std	47.0	3.2	1.2	51.3	506
P1	47.7	2.0	1.8	51.5	594
P2	47.3	2.2	1.8	51.2	538
P3	46.3	2.8	1.5	50.6	549
P4	45.7	2.4	3.4	51.4	531
P5	46.0	2.7	2.9	51.5	527

3.3.1. Polyacrylamide (P1)

P1 has acrylamide monomer units consisting of carbonyl and amine groups, which are considered to be active in inhibition of silicate. The effect of dosage level on silicious scale growth was studied. We have performed experiments where the dosage was varied from 20 to 400 ppm. Then soluble SiO₂ was measured after 24, 48 and 72 hours (Figure 3.6.). Those results were found to be comparable with control experiments. The results are given separately for different reaction times, below.

For 24 h, at 20 ppm dosage of P1 a evident increase is seen in inhibition efficiency on silicate formation with ~75 ppm soluble silica. At 60 ppm dosage an increase is seen in inhibitory efficiency with ~140 ppm soluble SiO₂. At 100 ppm dosage, an evident increase also is seen with ~180 ppm soluble SiO₂. By addition of 200 ppm and 400 ppm additive the inhibitory effectiveness is slightly enhanced. At 200 ppm inhibitor dosage level ~190 ppm and at 400 ppm dosage level ~195 ppm soluble silica is seen.

For 48 h, at 20 ppm dosage level, only marginally increase is seen with 14 ppm soluble silica. At 60 ppm, inhibition efficiency improved to ~40 ppm soluble silica and at 100 ppm similar marginal improvement is observed with ~55 ppm soluble silica. P1 have detrimental effect at 200 and 400 ppm on inhibitory efficiency (loss of ~30 and ~60 ppm soluble silica).

For 72 hours, with increase of P1 concentration, silicon concentration decreases but there is no remarkable difference in $[\text{Si}^{4+}]$. A regular decrease is observed with increase of additive dosage. P1 have detrimental effect at high inhibitor dosage. At 400 ppm, ~100 ppm loss of soluble silica was seen. As a result, P1 is more effective for 24 hours. For 48 and for 72 hours, inhibitor demonstrates reverse effect most probably due to flocculation.

Flocculation can be defined as the interaction of polymeric molecule with more than one colloids and as a result the precipitation of this hybrid structure. The mechanism of this process is schematically shown in Figure 3.5.

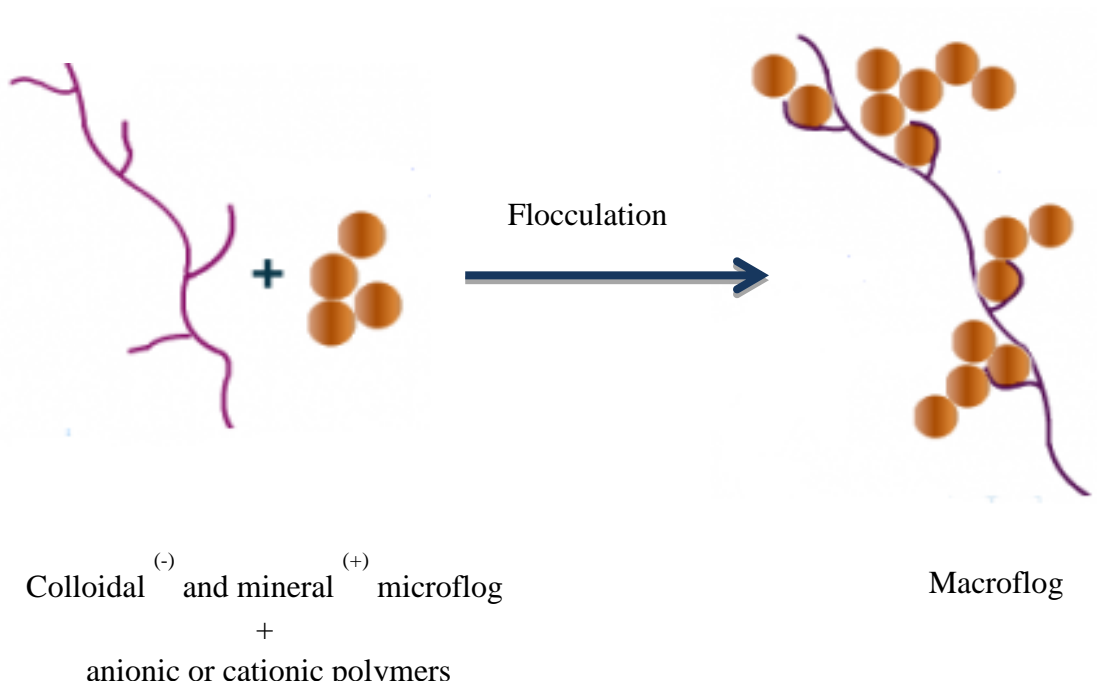


Figure 3.5. Schematic illustration of flocculation of silica and polymer chains.

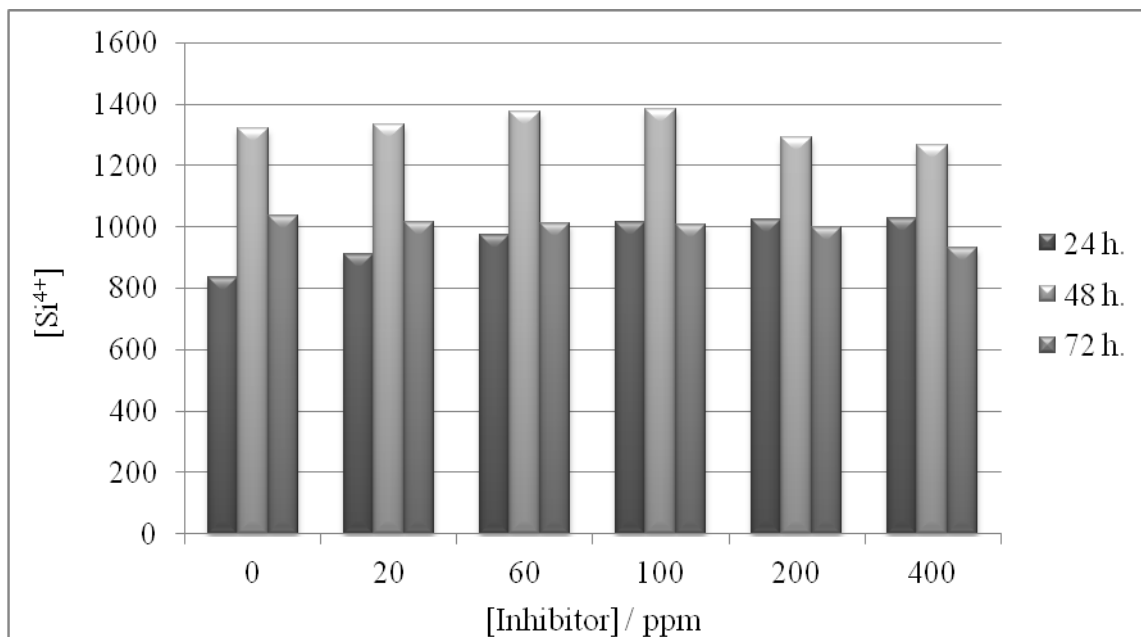


Figure 3.6. Silica solubility test of Polyacrylamide (P1).

In addition to silica concentration suspended in reaction mixture is studied for testing of inhibitors.

The effect of Polyacrylamide (P1) on solubility of metal are given in following in accordance with reaction times (Figure 3.7.). *For 24 h*, with increase in polymer dosage, metal concentration decreases. *For 48 h*, 20 ppm inhibitor concentration demonstrates effectiveness on enhancement of solubility of metal but after 20 ppm additive concentration, inhibitor does not show effectiveness. It has reverse effect after addition of 20 ppm polymer.

For 72 h, P1 provides increase on metal concentration at decantate. In 72 hours, at 20, 60 and 100 ppm inhibitor dosage, retains ~5, 6 and 5 ppm metal in decantate, respectively. It can be claimed that P1 shows dispersant effect; however, no chelating effect.

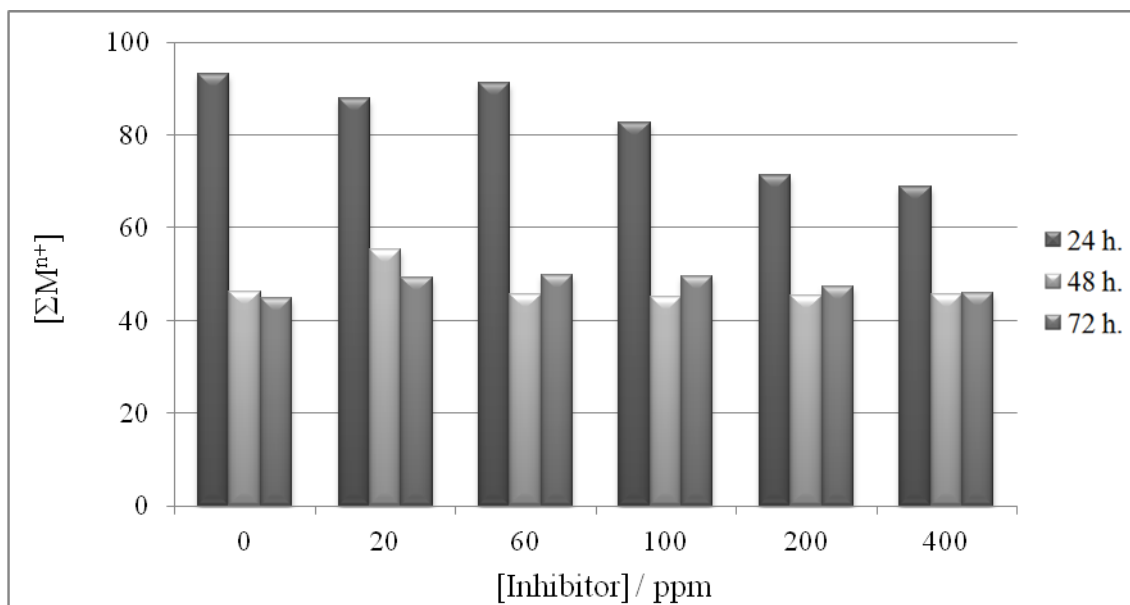


Figure 3.7. The effect of Polyacrylamide (P1) on solubility of metal.

Because P2 has low water solubility, high concentration solution could not be prepared, so it was not tested.

3.3.2. Poly(acrylamide-co-diallyl dimethyl ammonium chloride) (P3)

In addition to acrylamide, a copolymer of acrylamide and diallyl dimethyl ammonium chloride was also studied for inhibition. P3 includes carbonyl, amine and quaternary amine groups that are considered as active groups.

Figure 3.8. presents $[Si^{4+}]$ versus different inhibitor concentration. The results are explained below with respect to reaction times.

For 24 h, at 20 ppm additive of P3, effectiveness is seen but the inhibition efficiency appears indistinguishable from control (giving 8 ppm soluble silica). At 60 ppm, a clear increase is seen with ~70 ppm SiO_2 . 400 ppm inhibitor dosage causes a reverse effect on silica polymerization (loss of 64 ppm SiO_2). At 100 ppm and 200 ppm, inhibition efficiency drops (allowing ~30 ppm and ~8 ppm silica to remain soluble, respectively). Finally, 400 ppm additive level is detrimental to inhibition of silicate. It appears that additive dosage level has an important role on silica formation. Further dosage increase can cause a reduction in performance, especially over dosage of inhibitors that

has positive charge on the inhibitor molecules. In the case of P3, quaternary amine groups associate with negatively charged silica particles and insoluble silica-polymer composites form. On the basis of previous studies, charge density also is an important factor. A high positive charge density is detrimental to inhibition (Demadis and Stathouloupoulou 2008).

For 48 and 72 h, experiments, all inhibitory activity is lost on polymerization. As a result, P3 has better effect in short time.

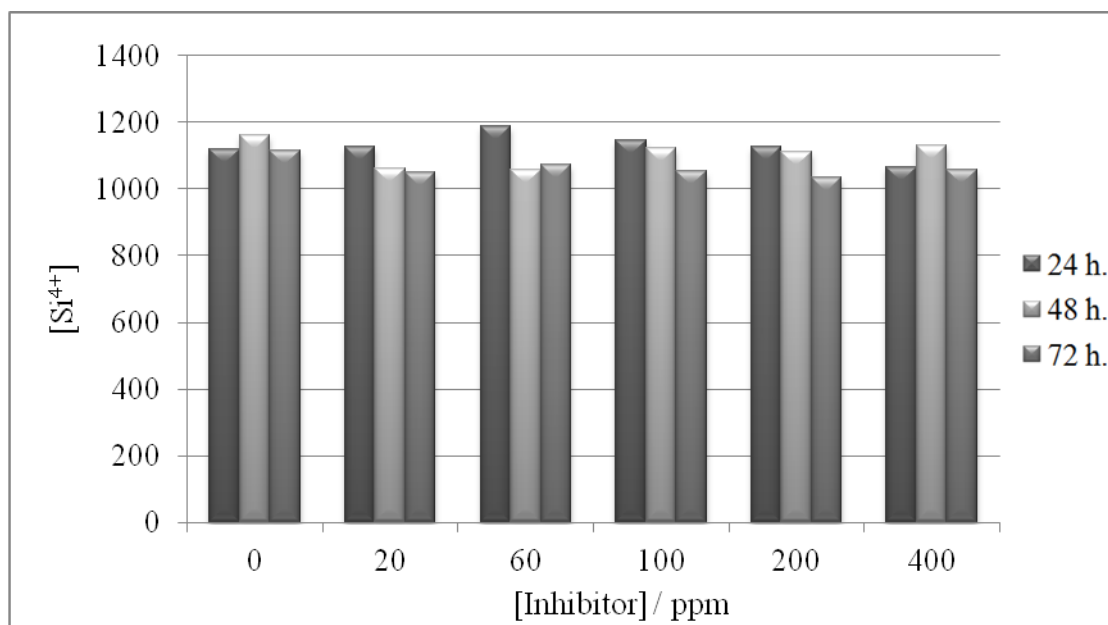


Figure 3.8. Silica solubility test of Poly(acrylamide-co-diallyl dimethyl ammonium chloride) (P3).

The effect of P3 on solubility of metal was examined (Figure 3.9.). The test results on solubility of metals and silica are not parallel each other. Polymer show effectiveness on inhibiting of polymerization reaction; however, it does not show inhibition activity.

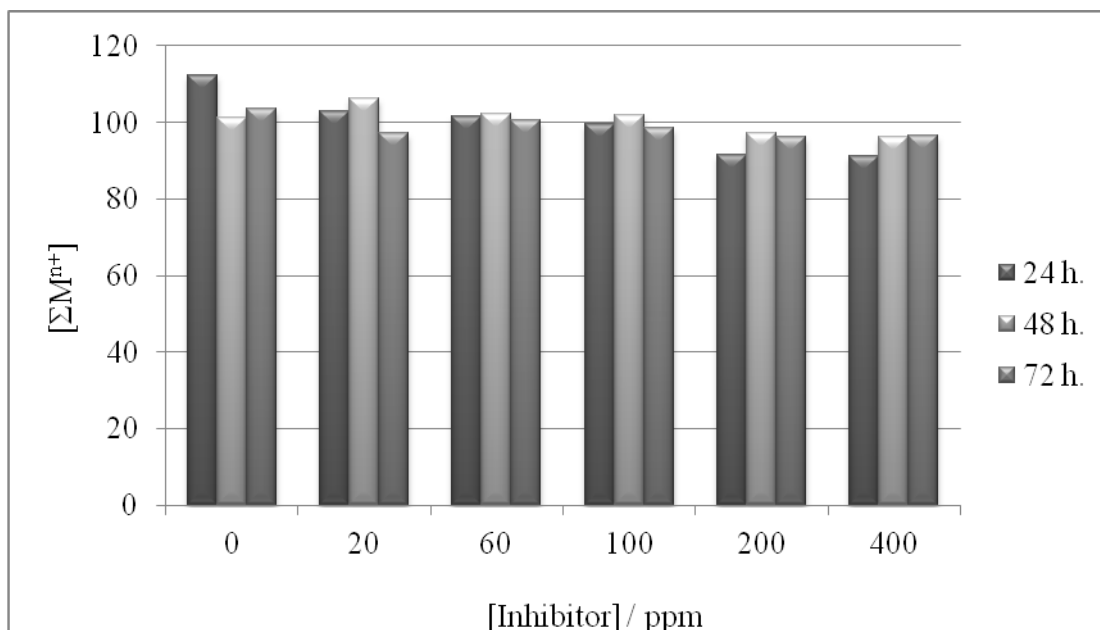


Figure 3.9. The effect of Poly (acrylamide-co-diallyl dimethyl amonium chloride) (P3) on solubility of metal.

3.3.3. Polyvinylpirrolidone (P4)

Polyvinylpirrolidone (P4) also were examined. Polyvinylpirrolidone is a water-soluble polymer made from *N*-vinylpyrrolidone monomers that include carbonyl groups. It is assumed that carbonyl groups act on inhibition of silica formation. Silica solubility test results of P4 are given in Figure 3.10. For 24, 48 and 72 hours, with additional inhibitor concentration, additional inhibitor performance is seen. By contrast with other inhibitors, further inhibitor dosage increase causes increase on inhibitory effect.

For 24 h, at 20 ppm dosage the concentration of soluble silica concentration is 50 ppm. At 60 ppm dosage of P4, an clear increase is observed (giving 150 ppm soluble silica). By 100 ppm addition of P4, an improvement is also seen on solubility of silica with 350 ppm soluble silica. At dosage of 200 and 400 ppm, an evident performance enhancement also can be seen (with 625 ppm and 650 ppm silica respectively).

For 48 h, the rise of inhibitor dosage is proportional to rise of soluble silica concentration. At 20 and 60 ppm, insufficient increase is seen (with 25 ppm and 50 ppm soluble silica, respectively). With further addition to 100 ppm, clear increase is seen

with 125 ppm silica concentration. Finally at 200 ppm and 400 ppm additive concentration a sharp increase is seen with ~750 ppm soluble silica.

For 72 h test results are parallel to 48 hours test results. At 20 and 60 ppm, $[\text{Si}^{4+}]$ is 25 ppm and 50 ppm, respectively. After 100 ppm a clear increase is seen. At 100 ppm dose level 225 ppm, at 200 ppm dose level 550 ppm and at 400 ppm dose level 625 ppm soluble silica is measured.

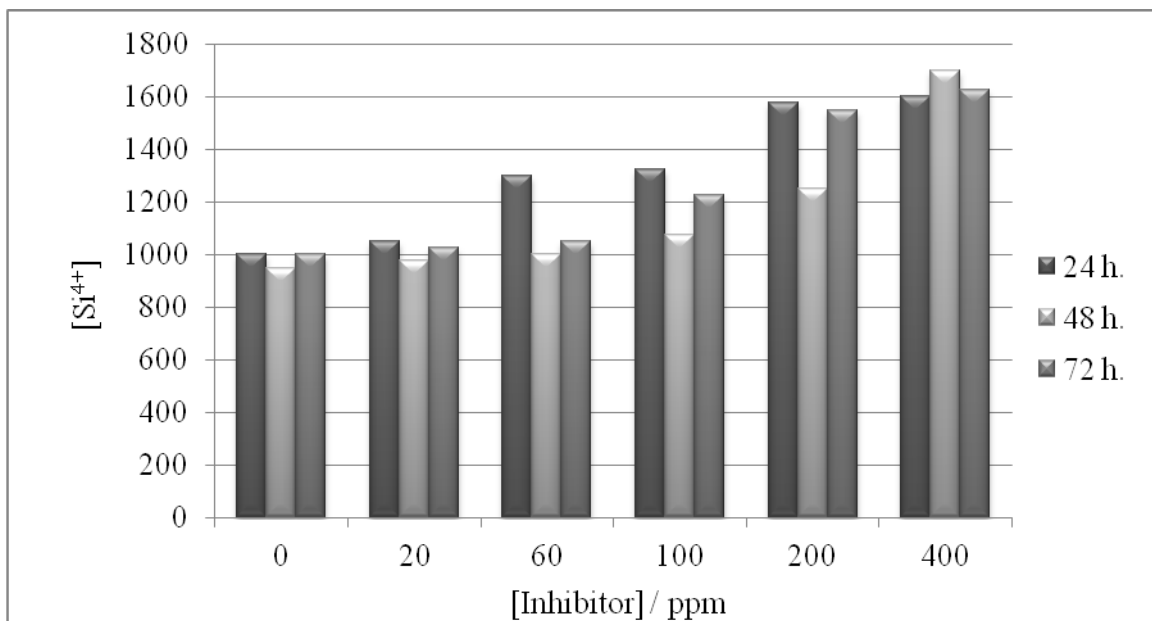


Figure 3.10. Silica solubility test of Polyvinylpyrrolidone (P4).

Metal solubility tests results of P4 don't show clear difference (Figure 3.11.). None of the P4 dosage provides better suspension of metal cation. It seems that P4 show efficiency only for silica, not metal cations.

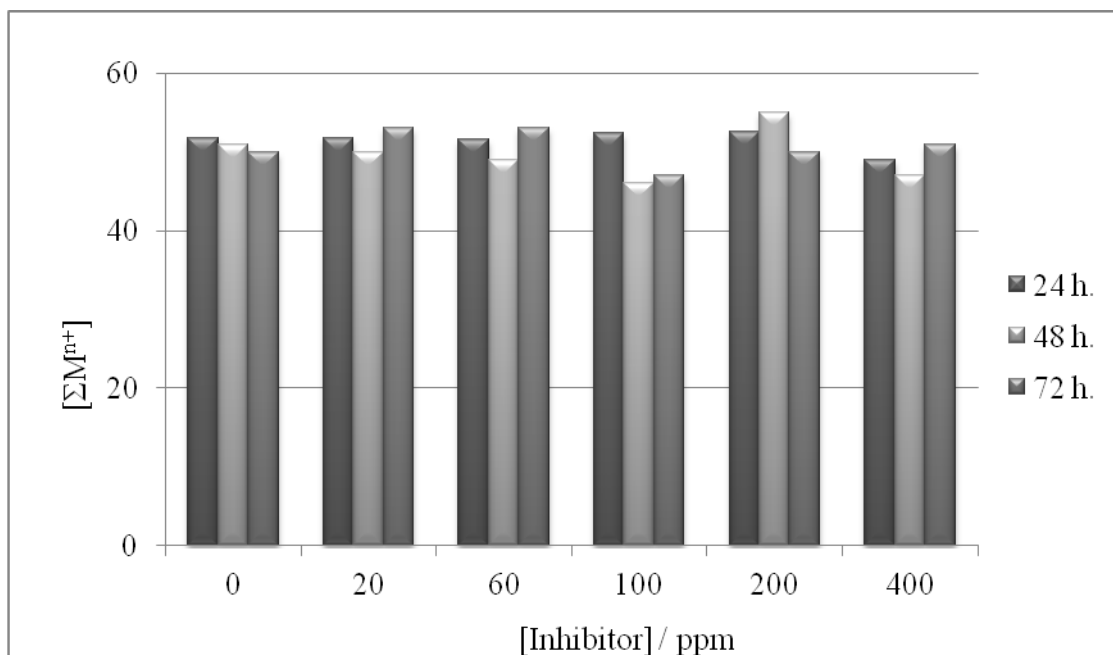


Figure 3.11. The effect of Polyvinylpyrrolidone (P4) on solubility of metal.

3.3.4. Polyacrylicacid (P5)

Polyacrylicacid is high molecular weight homopolymer of acrylicacid monomers. These acrylic acid monomers include polar acetic acid groups. Acetic acid groups considered to be active on silica formation. Silica solubility test of P5 were performed and the results are given in Figure 3.12. *For 24 h.*, when 60 ppm P5 is present in solution ~220 ppm dissolved silica is observed. At 100 ppm and 200 ppm inhibitor dosage, an enhancement on inhibition efficiency with ~180 ppm and ~170 ppm soluble silica was obtained. However, 60 ppm seems optimum concentration. At 400 ppm concentration, there is no remarkable difference.

For 48 h, 60 and 100 ppm inhibitor dosage level, provides approximately 60 ppm soluble silica. When dosage is 200 ppm, P5 show higher inhibitory activity with 80 ppm of soluble silica. Further inhibitor dosage increase to 400 ppm doesn't provides additional inhibition efficiency (30 ppm [Si⁴⁺]).

For 72 h, it was not observed regular increase or decrease on solubility on SiO₂. At 60 ppm, results are indistinguishable from the control experiment. 100 ppm additive is effective concentration with ~30 ppm soluble silica. Soluble SiO₂ drops at higher rate of additive dosage compare to the 100 ppm. A general observation is that

400 ppm additive of P5 has reverse effect on polymerization reaction (loss of 50 ppm $[\text{Si}^{4+}]$) most probably due to flocculation. Effective inhibitor concentration changes with experiment time. Whereas for 24 hours experiment 60 ppm is the most effective concentration, for 48 hours 200 ppm and for 72 hours 100 ppm inhibitor concentration is the most effective concentration. This may indicate that inhibition effect of P5 is better than its dispersant effect.

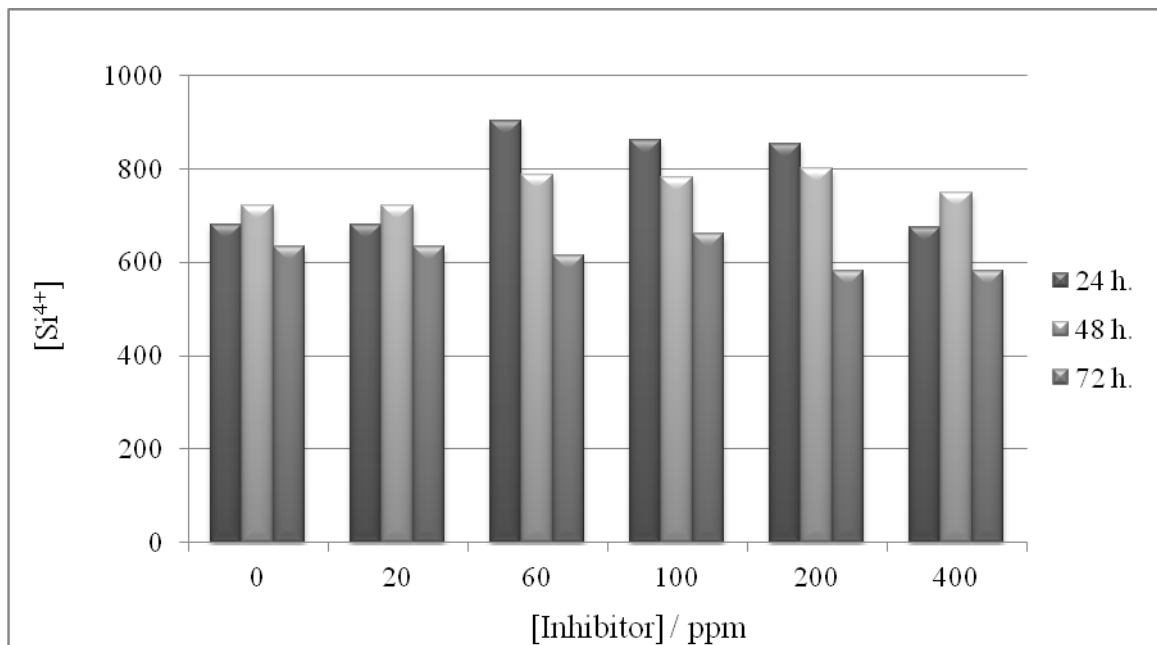


Figure 3.12. Silica solubility test of Polyacrylic acid (P5).

When the change on cation concentration is analysed compared to standart. A regular increase or decrease wasn't observed (Figure 3.13). One can conclue that P5 doesn't interact with cations.

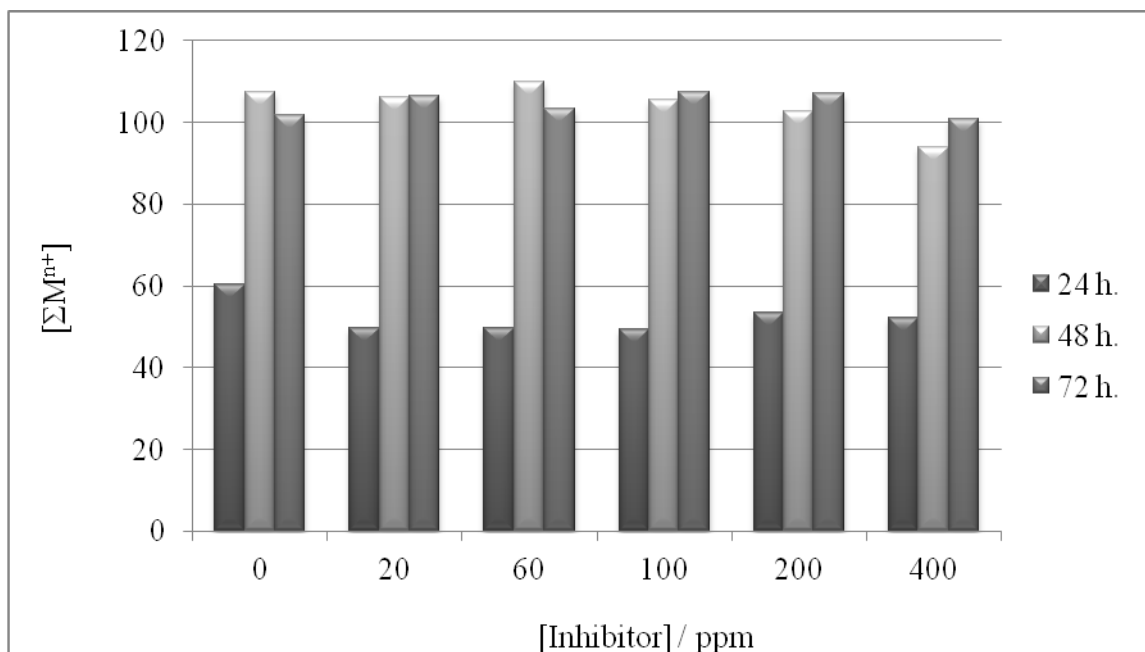


Figure 3.13. The effect of Polyacrylic acid (P5) on solubility of metal.

3.3.5. Molecular Weight on Parameter

In addition to time and concentration experiments, effect of molecular weight on silicate scale growth was examined. Polyvinylpyrrolidone (PVP) (P4), Polyethyleneglycol (PEG) and Polyacrylamide-co-acrylic acid (PAAMAA) were examined. Polyethyleneglycol (PEG) is a polymer that consist of ethylene oxide units $(-(O-CH_2-CH_2)_n-)$. PEG is also known as polyethylene oxide (PEO) or polyoxyethylene (POE). Polyacrylamide-co-acrylic acid (PAAMAA) is a water soluble macromolecule. It is co-polymer of acrylamide and acrylic acid. All polymers were examined at identical conditions: the dosage is 100 ppm and reaction time is 24 h.

Four different molecular weight of PVP on silicate scale growth were compared. According to silica solubility test results, with molecular weight increase up to 55.000/ Da effectiveness of PVP increase (Table 3.5.). It is seen a regular increase on soluble silica concentration with increase of molecular weight. By addition of PVP-1 soluble silica level is virtually same with control (4 ppm soluble silica increase). With increase on Mw to 10.000 Da effectiveness of inhibitor also increase. By addition of PVP-2, retains 11 ppm soluble SiO_2 . PVP-3 (40.000 Da) has better inhibition effect on silica

polymerization with 20 ppm soluble silica. Finally, 38 ppm soluble silica retains by addition of PVP-4 (55.000 Da).

Table 3.5. Solubility test of PVP on metals and silica. (All units are given in terms of ppm.).

	Mw / Da	[Mg²⁺]	[Ca²⁺]	[Fe²⁺]	[ΣMⁿ⁺]	[Si⁴⁺]
STD		46	3	41	91	1320
PVP 1	8.000	50	2	45	96	1324
PVP 2	10.000	47	2	43	93	1331
PVP 3	40.000	48	2	45	95	1340
PVP 4	55.000	49	3	45	97	1358

Two different molecular weight of PEG were compared in respect to inhibitory activity. Solubility test of PEG polymers are represented in following (Table 3.6.). It is seen in test results that PEG-2 works better than PEG-1. PEG-1 provides 145 ppm soluble silica and PEG-2 provides 184 ppm soluble silica at 100 ppm dosage level. Namely, longer chain of PEG is better inhibitor. The results of metal solubility analyses are parallel to silica solubility values. These polymers have moderate inhibitory activity.

Table 3.6. Solubility test of PEG on metals and silica. (All units are given in terms of ppm.).

	Mw / Da	[Mg²⁺]	[Ca²⁺]	[Fe²⁺]	[ΣMⁿ⁺]	[Si⁴⁺]
Std		46	3	40	90	1334
PEG-1	2000	47	3	47	97	1479
PEG-2	6000	49	3	54	106	1518

Solubility test of PAAMAA on metals and silica are given in Table 3.7. These results indicate that polymers that have much more high molecular weight can have weak effect on polymerization reaction. Results of metal solubility analyses of PAAMAA experiments don't show clear difference. When PAAMAA-1 was added, marginal increase was observed with ~12 ppm soluble silica. On the other hand, PAAMAA-2 provides 139 ppm soluble silica. It can be claimed that, excessive molecular weight of polymer can lose inhibitory efficiency. Because of excess length, polymer chains can interact each other and precipitate, i.e. flocculation takes place.

Table 3.7. Solubility test of PAAMAA on metals and silica. (All units are given in terms of ppm.).

	Mw / Da	[Mg²⁺]	[Ca²⁺]	[Fe²⁺]	[ΣMⁿ⁺]	[Si⁴⁺]
Std		46	3	40	89	749
PAAMAA-1	5.000.000	46	4	43	93	761
PAAMAA-2	200.000	45	3	42	89	888

Hydroxy Phosphono Acetic Acid (HPAA) acid was tested with its different concentration. With increasing inhibitor concentration, concentration of cations in decantate increase. The results indicates that 60 pmm of HPAA provides increase in inhibitor efficiency (Table 3.8.). However, differences are not distinctive. UV measurements (200-800 nm) of experiment of HPAA at different concentration also were done (Figure 3.14.). However, the change on % transmission with concentration of HPAA could not seen by direct measurement. Spectrophotometric method should be used. Indeed, it can be claimed that precision is high.

Table 3.8. The effect of HPAA on metal concentration. (All units are given in terms of ppm.).

[HPAA]	[Mg ²⁺]	[Ca ²⁺]	[Fe ²⁺]	[ΣM ⁿ⁺]
0	24.6	1.6	22.0	48.2
10	25.3	1.2	22.1	48.6
20	23.8	1.2	23.7	48.7
30	22.4	1.3	25.4	49.0
60	21.8	1.8	29.1	52.7

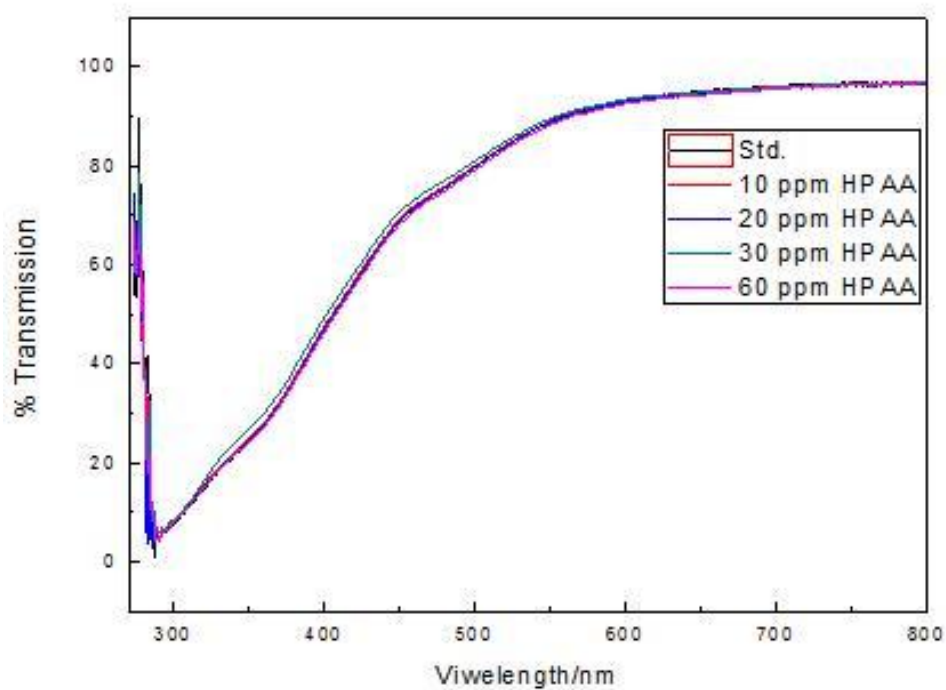


Figure 3.14. The change on % transmission with concentration of HPAA.

CHAPTER 4

CONCLUSION

Scaling is one of the important problem in geothermal fields. There are various inhibitors available in the market; however, the chemistry of inhibitors varies depending on type of deposits. Each field has its own inhibitor. Testing of the commercial and potential inhibitors in real geothermal system is costly in terms of time and budget wise. This is because testing of inhibitors at laboratory scale play key role. In this study, testing of potential silicate inhibitors was performed. As a methodology, first artificial scale was synthesized in the laboratory. The electron microscopy, X-ray diffraction, and elemental composition results suggest that artificial scale is similar to natural one obtained from Tuzla region, which has highly saline brine and metal siliceous deposit. Different polymeric molecules with different molecular weights and concentrations were studied at different reaction time. The chemistry of polymers are Polyacrylamide, Poly (vinyl sulfate, Potassium salt), Poly (acrylamide-co-diallyl dimethyl amonium chloride), Polyvinylpyrrolidone, Polyacrylic acid, Polyethylene glycol, Polyacrylamide-co-acrylic acid. All polymers have somehow inhibition to silicate scaling.

Polyacrylamide (P1) dissolves silica with the best performance at 100 ppm dosage. For 24 hours ~180 ppm and for 48 hours ~160 ppm silica dissolves. Yet, for 72 hours it doesn't have inhibitory effect.

Poly(acrylamide-co-diallyl dimethyl amonium chloride) (P3) has better performance at 60 ppm for 24 hours with ~70 ppm dissolved silica. For longer reaction time, difference is not significant.

Polyvinylpyrrolidone (P4) demonstrates additional inhibitor performance with further addition. With increase at additive dosage, dissolved silica concentration increase regularly. It is seen that 400 ppm additive is the best concentration with ~ 650 ppm dissolved silica for 24 hours. In contrary to other polymers further increase on inhibitor concentration, soluble silica concentration increase, as well.

Polyacrylic acid (P5) shows better effect at 60 ppm for 24 hours with ~180 ppm dissolved silica, at 200 ppm for 48 hours with ~80 ppm dissolved silica and at 100 ppm for 72 hours with ~30 ppm dissolved silica. The increase on dissolved silica

concentration is higher for 24 hours. It can be said that it's inhibitory effectiveness better than it's dispersant effect.

Because of low water solubility of P2 it was not tested.

As a result of this study we gain some experience and information about inhibitors. All of them have inhibition activity; however, none of them can be suggested as promising one because silica formation is complex mechanism. The results of this study would give rise to a new molecular design for inhibition.

REFERENCES

- Arnórsson, S. (1989). Deposition of calcium carbonate minerals from geothermal waters — theoretical considerations. *Geothermics*, 18(1–2), 33–39. doi: [http://dx.doi.org/10.1016/0375-6505\(89\)90007-2](http://dx.doi.org/10.1016/0375-6505(89)90007-2)
- Baba, A. (2003). Geothermal environmental impact assessment with special reference to the Tuzla Geothermal Area, Canakkale-Turkey. *Geothermal Training Programme Book*. Iceland: 75–114.
- Baba, A., and Ozcan, H. (2004). Monitoring and evaluation of the geothermal fluid on soil and water in the Tuzla geothermal field by GIS. *Remote Sensing and GIS for Environmental Studies*. 113:138–143.
- Baba, A., Ozcan, H., and Deniz, O. (2005). Environmental impact by spill of geothermal fluids at the geothermal field of Tuzla, Canakkale-Turkey. In *Proceedings of the World Geothermal Congress 2005* (April 24–29, 2005, Antalya, Turkey), 1–8.
- Baba, A. and Ármannsson, H., (2006). Environmental Impact of the Utilization of Geothermal Areas. *Energy Sources*, 1:267–278.
DOI: 10.1080/15567240500397943
- Baba, A., Yuce, G., Deniz, O. and Ugurluoglu, D. Y. (2009). Hydrochemical and Isotopic Composition of Tuzla Geothermal Field (Canakkale-Turkey) and its Environmental Impacts. *Environmental Forensics*, 10:2, 144–161. DOI: 10.1080/15275920902873418
- Bergna, H. E. (1994). Colloid Chemistry of Silica - an Overview. *Colloid Chemistry of Silica*, 234, 1–47.

- Benevidez, P. J., Mosby, M. D., Leong, J. K. and Navarro, V. C., (1988). Development and performance of the Bulalo geothermal field. Proc. 10th NZ Geothermal Workshop, Auckland, pp. 55-60.
- Demadis, K. D. (2003). Water treatment's 'Gordian Knot'. *Chemical Processing*, 66(5), 29-34.
- Demadis, K. D., & Mavredaki, E. (2005). Green additives to enhance silica dissolution during water treatment. *Environmental Chemistry Letters*, 3(3), 127-131. doi: DOI 10.1007/s10311-005-0015-0
- Demadis, K. D., Raptis, R. G., & Baran, P. (2005). Chemistry of organophosphonate scale growth inhibitors: 2. Structural aspects of 2-phosphonobutane-1,2,4-tricarboxylic acid monohydrate (PBTC center dot H₂O). *Bioinorganic Chemistry and Applications*, 3(3-4), 119-134. doi: Doi 10.1155/Bca.2005.119
- Demadis D. K., Mavredaki,E., Stathoulopoulou, A., (2007). Industrial water systems: problems, challenges and solutions for the process industries. *Desalination*, 213, 38–46.
- Demadis K.D., Sci. and Tech. Ind. Water treatment, (2010).
- Demir, M. M., Baba, A., Atilla, V., & Inanli, M. (2014). Types of the scaling in hyper saline geothermal system in northwest Turkey. *Geothermics*, 50, 1-9. doi: DOI 10.1016/j.geothermics.2013.08.003
- Doğan, I., Baba, A., Demir, M.M., (2013). Scaling problem of the geothermal system in Turkey, *Geothermal Systems & Energy Resources of Turkey and Greece*, 3: 29, 225.
- Gallup, D. L. (1997). Aluminum silicate scale formation and inhibition: Scale characterization and laboratory experiments. *Geothermics*, 26(4), 483-499. doi: Doi 10.1016/S0375-6505(97)00003-5

- Gallup, D. L., Sugiaman, F., Capuno, V., & Manceau, A. (2003). Laboratory investigation of silica removal from geothermal brines to control silica scaling and produce usable silicates. *Applied Geochemistry*, 18(10), 1597-1612. doi: Doi 10.1016/S0883-2927(03)00077-5
- Gill, J. S. (1993). Inhibition of Silica-Silicate Deposit in Industrial Waters. *Colloids and Surfaces a-Physicochemical and Engineering Aspects*, 74(1), 101-106. doi: Doi 10.1016/0927-7757(93)80401-Y.
- Gunderson, R. P., Dobson, P. F., Sharp, W. D., Pudjianto, R. and Hasibuan, A., (1995). Geology and thermal features of the Sarulla contract area, North Sumatra, Indonesia. Proc. Worm Geothermal Congress, Florence, volume 2, pp. 687-692.
- Hayakawa, S., Tsuru, K., Ohtsuki, C., & Osaka, A. (1999). Mechanism of apatite formation on a sodium silicate glass in a simulated body fluid. *Journal of the American Ceramic Society*, 82(8), 2155-2160.
- Ketsetzi, A., Stathoulopoulou, A., & Demadis, K. D. (2008). Being "green" in chemical water treatment technologies: issues, challenges and developments. *Desalination*, 223(1-3), 487-493. doi: DOI 10.1016/j.desal.2007.01.230
- Mavredaki, E., Stathoulopoulou, A., Neofotistou, E., & Demadis, K. D. (2007). Environmentally benign chemical additives in the treatment and chemical cleaning of process water systems: Implications for green chemical technology. *Desalination*, 210(1-3), 257-265. doi: DOI 10.1016/j.desal.2006.05.050
- Murray, L. E., Rohrs, D. T., Rossknecht, T. G., Aryawijaya, R. and Pudyastuti, K., (1995). Resource evaluation and development strategy, Awibengkok field. Proc. Worm Geothermal Congress, Florence, volume 3, pp. 1525-1530.
- Mützenber, S. (1997). *Nature and origin of the thermal springs in the Tuzla area, Western Anatolia, Turkey*. In *Active Tectonic of Northwestern Anatolia — The Marmara Poly-Project*, eds. Schindler, C., and Pfister, M. Zurich, Switzerland: vdf Hochschulverlag AG an der ETH, 301–317.

- Neofofistou, E., & Demadis, K. D. (2004). Use of antiscalants for mitigation of silica (SiO₂) fouling and deposition: fundamentals and applications in desalination systems. *Desalination*, 167(1-3), 257-272. doi: Doi 10.1016/J.Desal.2004.06
- Stathouloupoulou, A., & Demadis, K. D. (2008). Enhancement of silicate solubility by use of "green" additives: linking green chemistry and chemical water treatment. *Desalination*, 224(1-3), 223-230. doi: DOI 10.1016/j.desal.2007.06.007
- Tarcan, G., (2012). *Jeokimya sempozyumu Sayfa 84-85*, Denizli.
- Tarcan, G. (2005). Mineral saturation and scaling tendencies of waters discharged from wells (>150°C) in geothermal areas of Turkey. *Journal of Volcanology and Geothermal Research*, 142:263–283.
- Zhang, B. R., Chen, Y. N., Li, F.T., (2011). Inhibitory effects of poly(adipic acid/amine-terminated polyether D230/diethylenetriamine) on colloidal silica formation. *Colloids and Surfaces A: Physicochemical and Engineering Aspects*, 385(11-19).